ROLE OF COLONIC EPITHELIAL CELLS IN SUSCEPTIBILITY AND SEVERITY OF *CITROBACTER RODENTIUM* INFECTION IN MICE

by

ELENA VLADIMIROVNA GART

DVM, Novosibirsk State Agrarian University, Novosibirsk, Russia, 2010

A THESIS

submitted in partial fulfillment of the requirements for the degree

MASTER OF SCIENCE

Department of Diagnostic Medicine/Pathobiology

College of Veterinary Medicine

KANSAS STATE UNIVERSITY
Manhattan, Kansas

2011

Approved by:

Major Professor
Sanjeev K. Narayanan

Copyright

Abstract

Acute diarrhea induced by *Escherichia coli* is an important illness in humans, especially in children under age of two in developing countries. *Citrobacter rodentium* is used as murine model for *E. coli* infection in humans because it causes ultrastructural changes in murine colonic epithelium comparable to lesions produced by enteropathogenic *E. coli* (EPEC) and enterohemorrhagic *E. coli* (EHEC). Adult mice of many strains develop self-limiting epithelial hyperplasia when infected, whereas adult C3H and FVB mice are highly susceptible to infection and demonstrate mortality rates between 60 and 100% two weeks after infection. These susceptible strains of mice also have higher bacterial translocation to mesenteric lymph nodes. In mice, the cause of death could be hypovolemia due to dehydration that may occur due to an increase in paracellular permeability as well as dysregulation of apical and basolateral ion transporting proteins. *C. rodentium* virulence factors resemble those of *E. coli* and are believed to primarily alter tight junctions of colonic epithelial cells. Effectors delivered via the type III secretory system have been associated with actin condensation and pedestal formation. The exact mechanisms of *C. rodentium* infection, as well as changes that occur *in vitro* as well as in the intestine of various strains of mice are not completely understood.

This study introduced a new *in vitro Ptk6* cell line for *C. rodentium* infection, which can also serve as a model for EPEC in humans. Effect of *C. rodentium* on colonic epithelial cells of susceptible and resistant mice was determined in *in vivo* study. *C. rodentium* attached to *Ptk6* colonic epithelial cells, inducing attaching and effacing (A/E) lesions and loss of monolayer integrity, which charachterizes this cell line as a relevant *in vitro* model of *C. rodentium* and EPEC infections. Murine studies revealed that *C. rodentium* induced more severe disease and 100% mortality in juvenile C3H mice whereas Swiss Webster (SW) mice expressed only

moderate morbidity. The colonic lesions and changes in barrier function of colonic epithelium were more prominent in C3H mice. This study determined potential targets in the murine colon that play role the establishment and the outcome of the infection, indicating multifactorial nature of *C. rodentium*-induced diarrhea.

This study identified host factors involved in the initiation of *C. rodentium*-associated diarrhea and the outcome of infection, which can be useful in developing of novel strategies for preventing and treatment of infectious colitis.

Table of Contents

List of Figures

List of Tables

Acknowledgements

I acknowledge my major professor Dr. Sanjeev Narayanan, and my graduate committee that included Dr. Bruce Schultz and Dr. Derek Mosier. I thank Greg Peterson, Amit Kumar, Sailesh Menon, Megan Lawrence, Vladimir Akoyev, Mikayla Boge, Megan Lawrence, Tracy Miesner, Lloyd Willard, Joel Sanneman and COBRE facilities for their help during this work (Kansas State University).

Chapter 1 - Literature review

Citrobacter rodentium is a highly virulent enteric pathogen of mice, and *C. rodentium* infection in mice is a model for enteropathogenic and enterohemorrhagic *E. coli* infections of humans. In mice, *C. rodentium* attaches to the apical surface of the colonic epithelium resulting in microvilli effacement, enterocyte hyperplasia and rectal prolapse. Discussed below are recent achievements in research related to *C. rodentium* pathogenesis and host response to the infection.

C. rodentium as a model for attaching and effacing diarrhea

Citrobacter rodentium (formerly *C. freundii* biotype 4280 and *Citrobacter* genomospecies 9) is a natural murine pathogen (89). In the 1960s two major *C. rodentium*-induced outbreaks of diarrhea that were associated with high morbidity and mortality occurred in mouse colonies, and there was one report of a similar outbreak in a guinea pig colony (98, 106). *C. rodentium* has high genetic and pathogenic similarity to enteropathogenic *E. coli* (EPEC), which causes multiple cases of diarrhea worldwide, primarily affecting children in developing countries. *C. rodentium* possess a locus of enterocyte attachment (LEE), which is similar to that in EPEC. Mice infected with *C. rodentium* exhibit attaching and effacing (A/E) lesions that closely resemble those induced by EPEC strains in other animals and humans (35, 47, 80, 115, 131, 137). Due to ethical reasons it is impossible to study *E. coli* pathogenesis in humans *in vivo.* Therefore several *in vitro* and *ex vivo* models are utilized (44, 104, 119). However, these models lack the complexity of *in vivo* host-bacterial interaction s. Studies of EPEC pathogenesis in large animals, such as cattle or pigs can be prohibitively expensive which makes the development of a mouse model quite attractive (121, 153). Regarding virulence in mice, *C. rodentium* colonizes mouse colon and induces greater colonic hyperplasia than EPEC, which develops a commensal

relationship in the mouse intestine (97). The fact that *C. rodentium* is a natural murine pathogen with tropism to the colonic epithelium suggests that this bacteria is an ideal model for EPEC infection in humans. The *C. rodentium* murine model can be used to study host-bacterial interactions and identify host defense mechanisms against A/E pathogens.

Virulence factors of *C. rodentium*

A number of *C. rodentium* virulence factors, including those that are necessary for A/E lesions formation, are encoded in chromosomal LEE. *C. rodentium* LEE contains 41 genes and encodes type three secretion system (TTSS) structural and effector proteins, the outer membrane adhesin intimin, translocators, and proteins whose function is unknown currently. The majority of the LEE genes are organized into five polycistronic operons (LEE1, LEE2, LEE3, LEE5, and LEE4). The LEE1, 2 and 3 operons encode transcriptional regulators and structural components of the TTSS. LEE4 encodes intimin and the translocated intimin receptor (Tir). LEE5 encodes additional structural, translocating and effector proteins of TTSS. The A/E lesion formation depends on the TTSS, which is a common virulence mechanism for animal and plant bacteria (7, 96, 112). The 19 structural and effector proteins essential for TTSS are mainly encoded in the LEE1, LEE2, and LEE3 operons. Structural proteins (EspA, EspD, and EspB) form organelles that deliver effector proteins (Tir, EspG, EspF, Map, and EspH) to the host cell. All TTSS translocators, as well as intimin, Tir (encoded by *eae* gene) and CesT (Tir chaperone) are required for actin-rich pedestals formation (36). The secreted protein encoded by *espB* is required for bacterial attachment to the cell monolayers and for pedestal formation (103). The EspI protein and Map are required for colonization and induction of colonic hyperplasia in mice, while EspF, EspG, and EspH are not necessary for *C. rodentium* virulence (90, 99).

The *C. rodentium* protein intimin (outer membrane adhesion protein) is the first product of the LEE that has been associated with A/E lesions. There are several classes of intimin, with the most common intimins α, β and γ. Intimin β is associated primarily with *C. rodentium* and influences host specificity and tissue tropism. *C. rodetium* intimin is required for intimate bacterial attachment to the cell surface and effective colonization of the mouse colon (101). Intimin binds directly to epithelial cells and interacts with host nucleolin and integrin. Intimin also binds to Tir, which connects attached bacteria to the cytoskeleton. During A/E infection, Tir is translocated from bacteria to the apical membrane of colonic epithelial cells. Once translocated, Tir binds to bacterial intimin inducing filamentous host cytoskeleton rearrangement, actin recruitment into pedestals, and an inflammatory response (31, 37, 46-48, 53). The Tir is important not only for bacterial colonization and induction of hyperplasia in mice, but also for long-term bacterial attachment to epithelial cells (37).

Among virulence factors of *C. rodentium* that are not encoded in LEE, the important role belongs to lymphostatin, which is encoded by the *lifA* (inhibitory factor A) gene (81). Lymphostatin is a 364 Da protein composed of two enzymes: glucosyltransferase and protease. Lymphostatin is essential in successful crossing of the intestinal epithelial barrier and colonization of extra-intestinal sites in mice. However, lymphostatin does not play role in formation of A/E lesions *in vitro* (83). The glucosyltransferase motif of lymphostatin decreases R_{TE}, increases paracellular flux of macromolecules and causes the redistribution of β-actin and tight junctional (TJ) proteins ZO-1 and occludin. Protease, in its turn, is responsible for redistribution of adherent junctional (AJ) proteins such as β-catenin and E-cadherin (9). Together the glucosyltransferase motif primarily affects TJs, whereas the protease motif predominantly disrupts the AJs. It has been reported that lymphostatin disrupts intestinal epithelial barrier *in*

vitro by modulating Rho GTPase activity: the glucosyltransferase motif suppresses Cdc42 activity, while the protease motif activates Rho, leading to disruption of TJs and AJs, respectively (82).

C. rodentium pili are also encoded outside the LEE and include type I and type IV pili. The initial adherence of *C. rodentium* to epithelial cells is mediated by the type IV pilus, which is encoded by the *CfcI* gene. Type IV pili, along with the inner membrane nucleotide binding protein, are required for initial adherence and colonization of mice with *C. rodentium* (99). The type I pilus has been identified recently and is similar to those of *Salmonella enterica* serovar Typhimurium instead of *E. coli* (29).

The stationary phase sigma factor RpoS is another virulence factor of *C. rodentium* encoded in LEE. RpoS is important for survival under stress conditions for many enteric bacteria (69, 78, 111). In *C. rodentium,* RpoS plays an important role in resistance to oxidative stress induced by H_2O_2 and facilitates heat tolerance. Expression of the major *C. rodentium* catalase, HPII (KatE), which protects bacteria from oxidative stress, is highly RpoS dependent. Production of virulence factors curli fimbriae and cellulose by *C. rodentium* is positively regulated by RpoS. While RpoS negatively affects *C. rodentium* growth in stationary phase *in vitro,* it is beneficial for successful bacterial colonization of mouse colon. RpoS controls transcription of the LEE genes, including LEE regulators; RpoS also regulates the amounts of LEE proteins that are secreted (41). Overall, in *C. rodentium,* RpoS is associated primarily with bacterial attachment and resistance to stress but it is not necessary for A/E lesion formation.

Like many other bacteria (6, 39, 143) *C. rodentium* uses quorum sensing (QS) for communication and regulation of gene expression. Gram-negative bacteria use autoinducer type 1 (AI-1), autoinducer type 2 (AI-2) and autoinducer type 3 (AI-3) signaling systems. The

signaling molecules of the quorum systems bind to their periplasmic receptors and activate QS responsive operons in the bacterial genome (8, 50). *C. rodentium* utilizes both AI-1 and AI-2 systems, although AI-2 system has only a minor role in *C. rodentium* virulence. The AI-1 system utilizes signaling molecule N-acylhomoserine lactone (92), which at high bacterial cell densities interacts with its cytosolic receptor LuxR inducing activation of virulence genes. Surprisingly, in *C. rodentium* the loss of AHL QS resulted in an increase of virulence (30).

Summarizing above, *C. rodentium* utilizes multiple virulence mechanisms necessary for change of morphology and physiology of host cells that eventually allow bacteria to disseminate, infect, and colonize mouse intestine and distant internal organs.

Transepithelial ion transport and transepithelial electrical resistance

A/E pathogens colonize the gastrointestinal (GI) tract, particularly the intestine,to induce multiple types of damage to the epithelium and subepithelial layers. Studying pathogen-host interactions during A/E infection, it is important to remember that the intestine has regional specialization, which is associated with presence of distinct cell types in different areas. Water movement in the intestine occurs paracellularly or transcellularly. In the colon, water absorption is facilitated by specialized water channels called aquaporins and to some extent through ion transporters (84) . Ion transporters and channels are distributed in the enterocyte asymmetrically, and their coordinated activity is important for water and solute movement (94). The primary driving force for ion absorption and secretion is Na^+/K^+ ATPase, which is located in the basolateral membrane of enterocytes. The Na^+/K^+ ATPase moves 3 Na^+ out of the cell in exchange for 2 K^+ entering the cell, causing polarization of the cell membrane (54). Water absorption is linked to Na^+ transport from the apical to basolateral membrane. Sodium enters the

cell from the apical membrane Na^+/H^+ exchanger NHE3 and via the apical epithelial sodium channel (ENaC) (150). In the enterocyte, SLC26A3 (also known as DRA – downregulated in adenoma or CLD - chloride losing diarrhea) an apical anion antiporter facilitates Cl^- movement into the cell in exchange for bicarbonate; bicarbonate is synthesized inside the cell from water and CO_2, as well as uptaken basolaterally (11, 54). Water secretion in the intestine is linked to chloride transport from blood to lumen. Chloride enters the enterocyte through the electroneutral $Na^+/K^+/2Cl^-$ cotransporter NKCC1, which is located at the basolateral membrane. K^+ exits the basolateral membrane through potassium channels, which increases cell membrane potential difference and in its turn leads to chloride exiting through the apical CFTR (cystic fibrosis transmembrane conductance regulator) channel. Bicarbonate can also exit the cell through the CFTR (11).

Diarrhea results from an imbalanced absorption and secretion of water and ions across the intestinal epithelium. Diarrhea benefits enteric pathogens by promoting their dissemination and infection of new hosts. In *C. rodentium*-induced diarrhea, host passage increased bacterial virulence in mice (18). It has been shown that unlike *Shigella* (73), which increases Cl^- secretion via the CFTR and induces secretory diarrhea, the EPEC infection minimally affects chloride secretion (68). In fact, EPEC-induced infection in Caco-2 cells was characterized by decreased epithelial levels of SLC26A3 and therefore reduced chloride absorption (57). The same study determined that downregulation of SLC26A3 by EPEC depended on effectors and translocators proteins of EPEC TTSS (57). The decrease of water absorption during EPEC infection has been linked to the downregulation of NHE3 in enterocytes (67), which is induced by EspF protein of TTSS (72). Recent *in vivo* studies demonstrated that *C. rodentium* infections of C3H and FVB mice result in profound decreases in RNA coding for DRA (22) and high mortality levels. When

animals were given fluid therapy, mortality was reduced without affecting intestinal inflammation. The same group earlier performed genome-wide transcriptional analysis of FVB and SW mice to identify candidates that may contribute to the more severe diarrhea observed in susceptible mice (20). This study determined that among 5,123 differentially expressed genes between SW and FVB mice, a large proportion belonged to those involved in intestinal ion transport and its regulation. Hence, A/E pathogens decrease DRA and NHE3 activities leading to decreased NaCl and water absorption, which leads to high amount of water in the bowels and eventually diarrhea.

Taken together, the evidence available suggests that disturbed ion secretion and absorption have significant effects on the severity of diarrhea induced by the murine pathogen *C. rodentium*. The underlying mechanisms that can prevent water loss remain to be defined.

Apical junctional complex and its role in A/E infection

Under normal conditions the colon is involved in both water absorption and secretion through crypts and surface epithelium. Proximal and distal colons efficiently absorb water through leaky and moderately tight epithelium, respectively. The difference between leaky and tight epithelium lies in the ratio of paracellular to transcellular resistance. In the leaky epithelium transcellular resistance is greater than paracellular, while in tight epithelium paracellular resistance is about 1000 times larger than transcellular. In mouse colon the paracellular resistance is 23 times higher than the transcellular, and crypt epithelium is thought to be "moderately" tight (58). Epithelial cells in colon have different degrees of proliferation and differentiation, thus cells in crypts differ from cells at the epithelial surface. The transepithelial electrical resistance of crypts is 3 times higher than that of surface epithelium, but the

transcellular resistances do not differ between surface and crypt epithelium (58). Hence, the leakiness of the surface epithelium is determined by the high density of ion channels which determines its low transcellular resistance.

Epithelial cells are sealed to each other by apical junctional complex (AJC), which is defined as a highly specialized structure near the apical aspect of the lateral membrane of polarized epithelial cells. This complex regulates adhesion between neighboring cells and plays an important role in intestinal epithelial barrier function. The AJC is also important for signaling pathways controlling cell proliferation, cell differentiation and cell polarity (38, 45, 136, 148). AJC consists of TJs, AJs and desmosomes (135).

The AJs connects cells and regulates tissue formation and morphogenesis during development and maintenance of solid tissues in the adult organism (42). The cadherins and catenins are the major cell adhesion molecules at AJs. Cadherins connect cells though hemophilic interactions and are linked to the cell cytoskeleton through catenins (95). Cadherins and catenins are required for cell-cell adhesion, as their function cannot be replaced by other AJC molecules (42). The other AJ molecules, which facilitate cell-cell attachment, are nectins. Nectins influence E-cadherin-mediated adhesion, contributing to the strength of cell-cell adhesion. Both, nectins and cadherins can activate Cdc42 and Rac1 small GPTases. All nectins are connected to afradin, which directly interacts with the actin cytoskeleton (95, 139).

In epithelial cells, TJs form a continuous structure that separates the apical and basolateral plasma membrane compartments. TJs are composed of at least 40 different proteins, including occludin, claudins, zonula occludens (ZO) protein complex and junction associated adhesion molecules (59, 145) (Table 1-1). The ZO protein complex is composed of ZO-1, ZO-2 and ZO-3 proteins, which interact with F-actin, claudins and occludin, providing the link

between actin cytoskeleton and TJs. ZO proteins can also shuttle to the nucleus to regulate cellular proliferation and differentiation. Occludin serves as a marker of TJs, and its over-expression was linked to increased transepithelial electrical resistance (R_{TE}) (10), however, lack of occludin does not influence the ability of epithelia to form a polarized barrier, suggesting that occludin does not play a major role in establishing a paracellular barrier (109, 110). It is believed that occludin plays a role in epithelial permeability by incorporating itself into the claudin-based strands (45, 118). Recent studies have shown that occludin forms a semi-permeable pore in Caco-2 monolayers (derived from human intestine), regulating paracellular flux of large size molecules through the non-restrictive large channel pathway (3).

Claudins form the structural backbone of TJs. So far 24 members of the claudin family have been identified. Claudins are expressed in a tissue dependent manner. For example, colonic epithelial cells express claudins 1-5, 7, 8, 10, 12, 13, 15 and 19 (45, 118). Claudins not only contribute to R_{TE} (5, 13, 125), but also form a selective permeability barrier by forming size- and charge-selective pores for smaller size molecules (< 4 Å (5)) (133, 138). The first extracellular loop of claudins creates an electrostatic selectivity filter to control resistance and charge selectivity of the pores (permselectivity). A total of 15 claudins have been tested for their influence on monolayer permeability (Reviewed in (5)). Claudins 2 and 10 tend to make tight monolayers leakier. Claudins 1, 4, 5, 7, 8, 11, 14, 15, 16, 18 and 19 tend to make leaky monolayers tighter. Claudins 2, 15, 16, and 19 enhance permeability of cations, while Claudin-10 is selective for anions. It is believed that claudins interact with each other in an additive fashion, consistent with the idea that claudins form heterotypic pores (74).

Bacterial pathogens have an ability to interfere with structural components of the AJC, which can lead to barrier defects in the epithelium. These changes can have negative

consequences for the host while benefiting the microbe by enabling it to establish itself, gain nutrients and replicate (136). Inflammation plays an important role in the modulation of intestinal epithelial TJ barrier. Most pro-inflammatory cytokines, including interferon gamma (IFN-γ), tumor necrosis factor-alpha (TNF-α), interleukin (IL)-12 and IL-1β, cause an increase in TJ permeability, while some anti-inflammatory cytokines such as IL-10 and transforming growth factor beta (TGF-β) protect against the disruption of intestinal TJ barrier and development of intestinal inflammation (2). During *C. rodentium* infection TJs seem to be altered only when bacteria are intimately attached and inflammation persists, indicating the importance of direct bacterial contact for junctional disruption (63, 73). *C. rodentium* induces actin rearrangement into pedestals beneath adherent bacteria (37, 114, 131) and relocalizes claudin-3 (28), -1, and -5 from the lateral membrane into the cytoplasm in the colon epithelia (63). *C. rodentium* virulence factor lymphostatin plays role in disruption of AJC by changing the composition of ZO-1, occludin (9, 28), β-catenin and E-cadherin (9). In the murine cell culture model, CMT-93, derived from a murine renal carcinoma, *C. rodentium* increases paracellular permeability in a time dependent manner, relocalizes TJ proteins claudin-4 and claudin-5 towards the perinuclear space and downregulates their expression (44). In prediabetic NOD mice *C. rodentium* increases epithelial permeability and disrupts epithelial barrier function (85). Other mouse and *in vitro* models also exhibit increased epithelial permeability in response to *Citrobacter* infection (9, 28, 63). The functional and morphological changes that occur in AJC and TJs in response to A/E pathogens indicate their importance in establishment of A/E bacterial infection.

Understanding the network of junctional complexes and their involvement during *C. rodentium* infection will help development of new strategies to protect tissue barriers and to overcome the disease.

C. rodentium pathogenesis in mice

In infected mice non-specific clinical signs of *C. rodentium* infection include: ruffled coat, weight loss, depression (lack of appetite, reduced activity), malnutrition, perianal fecal staining, pasty dark feces, and dehydration (20-22, 100). Specific characteristics of the disease include transmissible murine colonic hyperplasia with limited inflammation and epithelial cell hyperproliferation in the descending colon (27, 33, 79, 89, 129). Commonly, mice get infected with *C. rodentium* via oral route, and it has been shown that in this case, *C. rodentium* colonization starts at the cecal patch. Later, as infection progresses, bacteria move to colon, and eventually heavily colonize it (142). The same study determined that 2 weeks after inoculation *C. rodentium* remains only at distal part of the colon and cannot be detected 3 weeks after inoculation. Hence, the cecal patch could be the site where *Citrobacter* adapts to the intestinal environment and activates the genes required for colonization.

The degree of inflammation during *C. rodentium* infection depends on age, diet, microbiota status and genetic background of mice. While *C. rodentium* causes diarrhea and rectal prolapse in mice of all ages, infection in adult mice is typically subclinical and self–limiting. In adult mice bacteremia and extra-intestinal infection are not hallmarks of infection, though recovery of bacteria from blood, liver and spleen has been reported (22, 75, 89). Weaning mice develop necrosis of the colonic mucosa and severe colitis and exhibit high mortality due to sepsis (12, 88). Genetic background plays an important role in susceptibility to *C. rodentium* infection. Inbred C3H and FVB mice are more susceptible to *C. rodentium* infection, and exhibit higher mortality when compared to C57BL/6, BALB/c, 129S1/SvImJ, or NIH Swiss mice strains. C3H mice are rapidly and heavily colonized by *C. rodentium* and undergo more rapid tissue pathology

than other strains. In C3H and FVB mice, higher numbers of bacteria are translocated to the mesenteric lymph nodes compared to relatively resistant strains (21, 130). In FVB mice, *C. rodentium* infection leads to epithelial cell hyperproliferation, severe inflammation, erosions, ulcers, and epithelial atypia (21). Susceptibility to infection does not depend on LPS responsiveness, but rather depends on regulation of ion transport in the colon (20). Fluid therapy fully protects C3H and FVB mice from mortality without affecting bacterial shedding, colon weight or histological colitis index (22). *C. rodentium* causes morphological changes in mouse colonic epithelium, characterized by A/E lesions (37, 47, 89, 114, 130), goblet cells depletion and reduced levels of MUC2 and trefoil factor 3 (Tff3) in the lumen (14). *Citrobacter* also disturbs kinetics of the colonic epithelia by modifying ion transport, especially the exchange of chloride and bicarbonate (20, 22). In summary, the severity of *C. rodentium* infection greatly varies between mice strains, while bacterial colonization is generally limited to the colon, where primarily epithelial cells interact with pathogen.

Host defense against *C. rodentium* infection

Host immune response to *C. rodentium* is complex, involving innate and adaptive immune defense mechanisms for bacterial clearance. Adaptive immune response involves T and B lymphocytes, which are critical for clearance of infection (131). Host response to *C. rodentium* is predominantly Th1-dependent, with increased numbers of $CD4^+$ T and $CD8^+$ T cells in the colonic lamina propria and epithelium, respectively (26, 70, 71). Induction of Th1 cytokines such as IFN-γ and IL-12 in colonic tissue is increased during *C. rodentium* infection, while the Th2 response and interleukin-4 (IL-4) are not (71). The deficiency in IFN-γ leads to deficient endocytosis, phagocytosis, and antigen-presenting cell activation in mice, resulting in a less

mature phenotype of these cell types (122). Th17 response is characterized by interleukin-23 (IL-23) production has been identified in response to *C. rodentium* (132). Lack of IL-17, IL-22 and IL-23 cytokines results in increased susceptibility to *C. rodentium* infection in mice (76, 92, 154). Among the factors produced by $CD4^+$ T and B cells, antibacterial IgG is particularly important for *C. rodentium* clearance (147), while $CD8^+$ T cells, IgA, and IgM do not seem to be play an important role (91, 123).

Several innate immunity factors have been recognized for their importance in *C. rodentium* infection. It has been shown that mucin-2 (MUC-2), secreted by goblet cells (64), limits intimate bacterial attachment to the epithelial cells (15). Inflammatory mast cells not only induce inflammation in response to *C. rodentium*, but they also have the capacity to directly kill *Citrobacter,* decreasing severity of hyperplasia and mortality (140). A recent study (56) determined that toll like receptor (TLR)-dependent signaling through myeloid differentiation factor (MyD) 88 is required for TNF-α and IL-6 production and maintaining mucosal integrity in response to *C. rodentium* infection. Additionally, it revealed that MyD88 activation promotes epithelial cell turnover and repair during *C. rodentium* infection. Antimicrobial peptides have diverse ranges of antimicrobial activity (49, 105, 151). Also, they were claimed to have additional biological functions such as wound repair mechanisms, chemo attractant properties that recruit inflammatory cells to inflammatory foci, induction of angiogenesis, interaction with LPS, and induction of cytolysis (86, 108). In mice cathelicidin-related peptide mCRAMP is produced in the colon with little expression in the small intestine and no expression in the stomach or liver (65, 66, 75). mCRAMP has antimicrobial activity against *C. rodentium* and decreases bacterial colonization and *C. rodentium*-induced pathological changes in colon at early stages of infection (75). Mucosal immunity is important for host defense against *C. rodentium;* it

involves various innate and adaptive mechanisms that regulate bacterial adherence, proliferation and clearance within colonic mucosa. Understanding the immune mechanisms that allows a host to prevent and overcome the disease can be the targets for preventive and therapeutic treatment of the EPEC in humans.

Probiotics decrease impact of *C. rodentium* infection

The mammalian GI tract is normally colonized by multiple species of endogenous microorganisms that play important roles in host nutrition and prevent intestinal disorders. Commensal intestinal bacteria, including lactic acid-producing bacteria, have been shown to have antimicrobial properties against A/E pathogens. *Bacillus subtilis* is commonly present in the GI tract of mice and humans. Inoculation of highly susceptible suckling NIH Swiss mice with spores of common GI tract resident, *B. subtilis,* one day prior to *C. rodentium* inoculation, reduces mortality rate and enteropathy in mice without affecting bacterial colonization of internal organs (33). Oral gavage of a *Lactobacillus rhamnosus* and *Lactobacillus helveticus* probiotic mix one week prior to and during *C. rodentium* infection prevents death in neonatal mice in the presence of T cells (52). *Saccharomyces boulardii* is thermophilic non-pathogenic yeast that has been used *in vivo* for both prevention and treatment of infectious and inflammatory intestinal diseases (19, 60, 61). Post inoculation treatment with *S. boulardii* reduces morbidity and ameliorates *C. rodentium*-induced colitis due to decrease in *C. rodentium* adherence and cytoskeleton rearrangements (144). These studies indicate the protective role of microbiota, which facilitates competitive exclusion of pathogenic bacteria. Future studies involving indigenous and probiotic bacteria should be considered in *C. rodentium* models of intestinal

inflammation, to evaluate them as potential candidates for treatment and prevention of A/E infections.

Conclusion

In this review, we described the multiple factors that affect the establishment, progression and outcome of *C. rodentium* infection. *C. rodentium* utilizes various virulence factors while interacting with the host, the majority of which are encoded in LEE. *C. rodentium* is a natural murine pathogen, with pathogenic properties highly similar to EPEC, which allows the *C. rodentium*-mice model to be used as surrogate to study EPEC-induced infections *in vivo*.

Although host-bacterial interaction during *C. rodentium* infection is complex, bacterial colonization is limited to the colonic epithelium. In infected mice *C. rodentium* induces mucosal inflammation, hyperproliferation of epithelial cells and A/E lesion. The infection compromises the integrity of the epithelial barrier resulting in change of epithelial permeability and R_{TE}. *C. rodentium* induces diarrhea and subsequent dehydration in infected mice, due to impaired ion transport across the epithelium. Finally, was recognized the importance of the host immune system, as well as the protective role of intestinal microbiota in preventing or clearing *C. rodentium* infection.

In next two chapters were investigated the novel aspects of *C. rodentium*-host interaction in *in vivo* and *in vitro* systems. The aim of the first study was to determine the changes that occur in conditionally immortalized colonic epithelial Ptk6 cells following exposure to *C. rodentium*. In that study was evaluated the ability of this cell line to serve as a new *in vitro* model for *C. rodentium* infection. The ability of *C. rodentium* to attach to Ptk6 cells, compromise monolayer barrier and induce structural and functional changes in the cell monolayer was evaluated. It has

been determined that *C. rodentium*-induced changes in Ptk6 cell monolayers greatly resembling those in EPEC, which allow us to use this cell line as *in vitro* model for EPEC infection in humans.

In the second study, were compared the changes induced by *C. rodentium* in the colonic epithelium of susceptible (C3H) and resistant (SW) mouse strains. *C. rodentium* was deliverd to the GI by intracecal injection, a novel method that allowed us to evaluate early changes following inoculation. More significant changes in the epithelial morphology (TJs), and function (gene expression, R_{TE}) were determined in C3H mice compared to SW, following *C. rodentium* inoculation. Our results indicated the complexness of mechanisms that can contribute to *C. rodentium*-induced diarrhea. In the conclusion, we summarized the key points of performed *in vivo* and *in vitro* studies, which reveal new aspects of *C. rodentium*-host interactions and establishment of a new cell culture model for *C. rodentium* infection.

Figures and Tables

Table 1-1 Proteins involved in formation and modulation of TJs. (Reviewed in Bauer *et al*, 2011)

Group:	Proteins involved:
Transmembrane proteins	
(a) Tetraspan proteins	Occludin, tricellulin/marvelD2, marvelD3, claudins (1-24)
(b) Single-span proteins of the immunoglobulin superfamily(IgSF) type	JAMs, CAR, CLMP, ESAM
(c) Non-IgSF type single span proteins	CRB3, Bves
Peripheral proteins	
(a) Adaptor or scaffolding proteins	ZO-1. ZO-2, ZO-3, MAGI-1, MAGI-3, CASK/LIN-2, AF-6/afadin, ASIP/Par-3, PALS1, PATJ, cingulin
(b) Signaling molecules	RhoA, Rac1, Cdc42, kinase-A, kinase-G, mitogen-activated protein kinases, phosphoinositide 3-kinase, ZAK, Raf-1, MLCK, PP2A, PP1, DEP-1, heterotrimeric G-proteins
(c) Transcriptional regulators	ZONAB, CDK-4, Apg-2, symplekin, Jun, Fos, C/EBP, p120 catenin (dual residency)

Chapter 2 - *Citrobacter rodentium* Causes Structural and Functional Alterations in Conditionally Immortalized *Ptk6* Colonic Epithelial Cells

Abstract

Citrobacter rodentium is a highly virulent enteric pathogen of mice and is an animal model for enteropathogenic and enterohemorrhagic *E. coli* infections of humans. In mice, *C. rodentium* attaches to the apical surface of the colonic epithelium resulting in effacement of microvilli, enterocyte hyperplasia, and rectal prolapse. The objective of this study was to investigate *Ptk6* cells as a potential model for *C. rodentium* infection in mice. A conditionally-immortalized cell line derived from a *Ptk6* null mouse colonic epithelium was used in these studies to evaluate structural and functional changes in eukaryotic cells following exposure to *C. rodentium*. Transepithelial electrical resistance significantly decreased while permeability of the cell monolayer to dextran increased after incubation with *C. rodentium*. Confocal microscopy of the monolayers revealed that there was disorganization of tight-junction proteins following 6-12 hours of bacterial exposure. Transmission electron microscopy showed bacterial attachment, pedestal formation, local disruption of tight junctions, and increased vacuolization. These results suggest that the capability of *Ptk6* cells to differentiate into absorptive, goblet, and endocrine cells, along with the characteristic changes they possess when exposed to *C. rodentium*, makes this cell line ideal for *in vitro* studies to define the cellular and molecular basis of its pathogenesis.

Introduction

Infectious diarrhea affects two to four billion people worldwide every year, with higher prevalence in children. In infants, enteropathogenic *E. coli* (EPEC) causes persistent watery diarrhea, often accompanied by insignificant fever and vomiting. In spite of high prevalence of EPEC-induced diarrhea in both developing and developed countries, the pathogenesis of EPEC remains poorly defined (73).

Citrobacter rodentium is a murine pathogen that can cause outbreaks of diarrhea in laboratory mice colonies (98, 106). Mice infected with *C. rodentium* exhibit attaching and effacing (A/E) lesions that closely resemble those induced by enterohemorrhagic *E. coli* (EHEC) and EPEC strains in other animals and humans. For this reason, *C. rodentium* is used widely as a murine model for human EPEC infection (80). Non-specific clinical signs of infected mice include: ruffled coat, weight loss, depression, stunting, perianal fecal staining, pasty dark feces and dehydration (100). Specific characteristics of the disease are transmissible murine colonic hyperplasia with limited inflammation and epithelial cell hyperproliferation in the descending colon. Degree of inflammation depends on age, diet, microbiota status and genetic background of mice (89). In infected mice, *C. rodentium* causes morphological and physiological changes in colonic epithelium by attaching to the host colonic epithelium, inducing effacement of microvilli, and formatting pedestals beneath the adherent bacteria (A/E lesions). Infection disturbs kinetics of the colonic epithelium by modifying ion transport, especially, the exchange of chloride and bicarbonate (130). Apical junctional complex (AJC) is a highly specialized structure at the apical tip of the lateral membrane of polarized epithelial cells. This complex regulates adhesion between neighboring cells and its tight junctional components (TJ) play an important role in intestinal epithelial barrier function (136). The disturbance of TJs is important in a variety of

diseases, including various bacterial infections, Crohn's disease, and ulcerative colitis (17). Bacterial pathogens, including *C. difficile*, *B. fragilis*, *C. perfringens* and *C. rodentium* can interfere with structural components of the AJC, which usually leads to barrier defects and disruption of the epithelial monolayer (136). The change in function of TJs induced by A/E pathogens can be measured by detecting transepithelial electrical resistance (R_{TE}). The changes in TJs function are usually characterized by a decrease in R_{TE} and an increase in paracellular flux of macromolecules such as mannitol and dextran (16). It has been shown that the A/E pathogen rabbit EPEC (REPEC) redistributes TJ proteins ZO-1, ZO-2, and occludin to recruit them into A/E lesions. Interestingly, REPEC TTSS effector EspF interacts directly with ZO-1 and ZO-2 but not with occludin or claudin in the first hour of infection. REPEC EspF is also important for increasing the actin pedestals length in RK13 rabbit kidney cells. In epithelial cells, actin physically binds to TJ proteins such as ZO-1 and occludin, and actin rearrangement may lead to loss of binding and subsequent disruption of molecular TJ structure (104, 120).

Recently, the murine rectal carcinoma CMT-93 cell line was evaluated as an *in vitro* model system for *C. rodentium* infection. *C. rodentium* was able to adhere to the CMT-93 monolayer, but in lower numbers than EPEC *in vitro* (44). Lower number of attached *C. rodentium* may be due to the fact that *C. rodentium* lacks bundle forming pilus that *E. coli* uses for initial binding (127). In CMT-93 monolayers *C. rodentium* increased paracellular permeability in a time dependent manner. In this model, disruption of the monolayer integrity was not apparent under light microscope. However, immunolabeling showed that claudin-4 and claudin-5 were relocalized towards the perinuclear space and their expression was down-regulated after infection. *C. rodentium* causes the upregulation of caspase-3-independent

apoptosis in CMT-93 cells, which was associated with cytosolic accumulation of apoptosis-inducing factor (44).

Murine colonic epithelial *Ptk6* cells, derived from a *Ptk6* null mouse, have characteristics of progenitor cells. When cultured on permeable fillers or on collagen gel the cells differentiate into villin-producing absorptive cells as well as a small number of goblet and neuroendocrine cells. Additionally, *Ptk6* cells form organoids when cultured in collagen gel. Growing in monolayer, these cells form domes when confluent and polarize to form a resistant barrier characterized by formation of TJs, which was confirmed by detection of ZO-1 and occludin (141). Studies on mice have shown that *C. rodentium* may utilize different strategies to compromise the intestinal barrier and induce diarrhea. These strategies include disruption of TJs, formation of A/E lesions, actin recruitment, and dysregulation of transepithelial water and ion transport. The objective of this study was to define the changes that occurred in *Ptk6* cells after challenge with *C. rodentium* and determine whether this cell line could be used as an *in vitro* model for studying *C. rodentium* pathogenesis.

Materials and methods

Cell culture

Mouse conditionally immortalized colonic epithelial cells *Ptk6* (generously provided by Dr. Whitehead from Vanderbilt University, Germany) were cultured in RPMI-1640 medium (Invitrogen, Carlsbad, CA), supplemented with 5% fetal bovine serum (FBS, Atlanta Biological, Norcross, GA), 1% of Antibiotic-Antimycotic (Invitrogen), 1 μg/ml insulin, 10^{-5} M thioglycerol, 10^{-6} M hydrocortisone hemisuccinate (Sigma-Aldrich, Saint Louis, MO) and 5 units/ml of mouse gamma interferon (Peprotech, Rocky Hill, NJ). Cells were incubated at 33°C and 5% CO_2. The

culture medium was changed every other day and the cells were passaged with TrypLE reagent (Invitrogen). For most studies, cells were grown for 10 days on 0.30cm^2 Transwell permeable support membranes (Corning Costar, Corning, NY) with 0.4-μm pores to form confluent monolayer and achieve transepithelial electrical resistance ≥ 3000 Ω×cm^2. In some experiments cells were grown in 6-well plates (Corning) until confluence was reached.

Infection of monolayers

Two hours prior to infection *Ptk6* cell monolayers were washed three times with warm RPMI-1640 and then incubated in RPMI-1640, supplemented with 5% FBS and no antimicrobials. Overnight cultures of *C. rodentium* ICC 180 (kindly provided by Dr. Shi, Kansas State University, US) were diluted 1:10 in Luria-Bertani (LB) broth and grown at 37°C until OD_{600} reached 0.6. Then bacteria were centrifuged at 3000×g for 5 min and the resulting pellet was resuspended in RPMI-1640 containing 5% of FBS. Bacteria (100 μl) were added to the apical surface of the monolayer to a final concentration approximately 5×10^8 colony–forming units/ml (CFU/ml), corresponding to a multiplicity of infection of 150 units, and were incubated for indicated lengths of time.

In vitro paracellular permeability

Transepithelial electrical resistance of the monolayer grown on Transwells was measured using EVOM epithelial volt-ohmmeter (World Precision Instruments, Sarasota, FL). Paracellular permeability was determined by using fluorescein isothiocyanate (FITC)-conjugated dextran of molecular weight 10 kDa, 40 kDa and 70kDa (Sigma-Aldrich). Dextrans were added to the apical compartment of each well at concentrations 1.25×10^3, 3.125×10^4 and 1.8×10^4 for 10kDa, 40kDa and 70kDa respectively and incubated at 37°C for an indicated duration (1 h or 3 h).

Monolayers treated with RPIM-1640 (contained 5% FBS) served to measure a baseline of dextran permeability in *C. rodentium*-untreated monolayers. Monolayers treated with 5 mM of EDTA (Ambion, Inc, Austin, TX) to disrupt cell-cell junctions, and measure the maximum amount of dextrans that call pass through disrupted monolayers. The solution from the basolateral side was then sampled, and the fluorescence determined immediately (485 nm excitation and 527 nm emission; Fluoroskan Ascent FL; Thermo Fisher Scientific, Waltham, MA). Standard curves were obtained by serial dilution (2.5 µg/µl to 25 pg/µl) of the FITC-dextrans.

Assessment of bacterial adhesion

Epithelial cells were grown in 24-well culture plate until a confluent monolayer was achieved to assess bacterial adhesion. Two hours prior to infection, monolayers were washed with sterile phosphate buffered saline (PBS: 137 mM NaCl, 2.7 mM KCl, 4.3 mM Na_2HPO_4, 1.47 mM KH_2PO_4, pH 7.4) and incubated with RPMI-1640 containing 5% BSA. Bacteria were added to the apical surface of the monolayers at concentration of 150 bacteria per cell and incubated at 37°C for 3 h. Cells were then washed three times to remove non-adherent bacteria, and treated with 0.5% Trypsin (Invitrogen) for 5 min. To enumerate invaded bacteria, part of the monolayers were treated with 100 µg/ml of gentamicin (Sigma-Aldrich) for 1 h, then washed and treated with trypsin. Cells were scraped into tubes, centrifuged, serially diluted, and plated onto LB plates containing kanamycin (50 µg/ml). Number of bacterial colonies (CFU) was recorded the following day.

Immunocytochemistry and confocal imaging

Monolayers were washed in PBS, fixed in 4% paraformaldehyde (Fisher Scientific International, Hampton, NH) for 30 min, quenched in 50 mM glycine in PBS and permeabilized in 0.5% TritonX (Sigma-Aldrich) for 30 min. Monolayers were then washed three times with PBS, three times with PBS containing 0.1% Tween 20 (Sigma-Aldrich) and saturated nonspecific binding sites (blocked) by incubating overnight in blocking buffer (PBS containing 5% bovine serum albumin (BSA, Sigma-Aldrich) and 0.1% Tween 20). Monolayers were incubated with primary antibodies (5 µg/ml) overnight, washed three times with PBS containing 0.1% Tween-20 and incubated with secondary antibodies in blocking buffer (10 µg/ml) for 2 h. If needed, tissues were stained for actin with phalloidin-594 (Invitrogen). Nuclei were counterstained with 4',6-diamidino-2-phenylindole (DAPI, Vector Laboratories, Burlingame, CA). To indicate the specificity of labeling, cells were labeled with secondary antibodies only, which resulted in lack of immunofluorescence (data not shown).

Monolayers were viewed by laser-scanning microscopy using similar intensities of red (543 nm), green (488 nm), and blue (364 nm) laser lights (LSM 510 Meta, Carl Zeiss, Göttingen, Germany). Transmitted light intensities were recorded and color images were generated by addition of red, green, and blue images. Each tissue section was centered manually using a 40× oil immers objective. Sections were scanned with resolution of 1024×1024 pixels per field (three fields per monolayer). During each scan, each line was scanned twice and averaged to remove noise. Each section was scanned sequentially, generating 70-90 images per stack. For each experiment, 9-12 stacks were acquired. Virtually superimposed images were obtained using software provided with the confocal laser scanning microscope (Aim, LSM 510 Meta, Carl Zeiss). Observations reported are based on at least three independent observations from three independent experiments.

Transmission electron microscopy

Monolayers incubated with *C. rodentium* were washed, fixed with modified Karnovsky's fixative (2% paraformaldehyde, 2.5% glutaraldehyde, 1.7 mM $CaCl_2$ in 0.1 M cacodylate buffer, pH 7.4), washed and post-fixed with 1% osmium tetroxide, embedded in Epon LX112 (EMS, Fort Washington, Pennsylvania) and then thin-sectioned on an Ultracut E-Reinchert-Jung ultramicrotome (C. Reichert Optische Werke AG, Vienna, Austria). Sections were stained with 5% uranyl acetate and 0.2% lead citrate and viewed with an electron microscope (Hitachi H-300, NY).

Quantitative real time RT- PCR

Prior to RNA extraction, *Ptk6* cells were grown on 0.30 cm^2 Transwell permeable support membranes for 10 days and then incubated with *C. rodentium* for 3h. RNA was extracted using TRIzol extraction. Briefly, cells were homogenized, pelleted, and supernatant was discarded. One ml of TRIzol Reagent (GIBCO, Invitrogen) was added to each sample and incubated for 5 min at room temperature. Then, 200 µl of chloroform were added to TRIzol, the mixture was shaken several times, and centrifuged for 15 min at 12,000 rpm. Clear upper phase was collected into new tube, mixed with 500 µl of ice cold isopropanol, incubated for 10 min at room temperature, and centrifuged for 10 min at 12,000 rpm. The resulting pellet was washed with 75% ice cold ethanol, and resuspended in 50 µl of distilled nuclease free water. Reverse transcription was completed for 30 mins at 50°C followed by 1 min of denaturation at 95°C. PCR amplification was continued for 40 cycles: 94°C for 15 sec (denaturation), 48-55°C for 30 sec (annealing) and 72°C for 30 sec (extension). Target genes used for RT-PCR analysis are listed in Table 1.

Data analysis

Analysis of variance, followed by Tukey's test was performed to compare mean differences in R_{TE} and dextran flux between vehicle-treated and *C. rodentium*-treated monolayers. The 90% confidence interval was calculated for the gene expression levels in *C. rodentim*-treated monolayers. Unchanged observations were within 90% CI for the observed values. GraphPad Prism version 5.00 for Windows (GraphPad Sofrware, San Diego, CA) or SAS version 9.2, (SAS, Cary, NC) software were used for statistical analysis. Data were presented as means±SEM, and differences were considered statistically significant when the probability of a type I error was < 0.05.

Results

C. rodentium adheres to and invades Ptk6 monolayer

Ptk6 cells formed polarized monolayer when grown on Transwell supports, they formed small number of mucin- and chromogranin-producing cells (data not shown), as it has been described (141), and possessed high R_{TE} (3629±101.8 $\Omega \times cm^2$).

Experiments determined that after 3 h of incubation the number of bacteria attached to the *Ptk6* monolayer reached the average of 21.36±2.24 CFU per cell, and invaded bacteria counts were less than 1 CFU per cell (0.246±0.024 CFU per cell).

Transmission electron microscopy determined that bacteria start attaching to the surface of the monolayer as early as 1h after inoculation (Fig. 2-1A). After 12 h incubation, numerous bacteria were attached to the cell surface (Fig. 2-1B). Bacterial attachment causes loss of microvilli at some regions of the cells and formation of membrane ruffling at the apical surface

of the cells. These structures are speculated to be actin-rich pedestals. In spite of pedestal formation, the overall cellular ultrastructure was not damaged (Fig. 2-1C).

Paracellular permeability of Ptk6 monolayers increases after treatment with C. rodentium

In order to determine if *C. rodentium* can increase the paracellular permeability, the change was measured in transepithelial electrical resistance of the monolayer as well as apical to basolateral flux of various sized dextrans. An intact *Ptk6* monolayer formed TJs and maintained an average R_{TE} of 3883±31.86 $\Omega \times cm^2$. After 3 h incubation with *C. rodentium* transepithelial resistance of the infected monolayer decreased significantly to 2107±201 $\Omega \times cm^2$ (Fig. 2-2A). Dextran flux increased in *C. rodentium* treated monolayers compared to untreated monolayers. Permeability to 10 kDa and 40 kDa dextran increased after 1h of 8.14×10^{-5} $\pm2.46\times10^{-5}$ and 5.59×10^{-5} $\pm2.49\times10^{-5}$cm/sec respectively in *C. rodentium*–treated monolayers. Dextran levels in vehicle-treated monolayers were lover detectable levels 1h after incubation. After 3 h of incubation, permeability of monolayers to 70 kDa dextran increased from 6.60×10^{-5} $\pm2.36\times10^{-5}$ cm/sec in vehicle-treated to 3.25×10^{-4} $\pm1.11\times10^{-4}$ cm/sec in *C. rodentium*-treated monolayers (Fig. 2-2B). Analysis of variance determined that *C. rodentium* treatment increased the permeability of monolayers ($P<0.05$), however, the size of dextrans and the length of treatment did not effect the permeability.

C. rodentium induces actin pedestal formation and disruption of occludin in Ptk6 cells

Actin and occludin formed a reticular pattern in vehicle-treated monolayers, characteristic of epithelial cells. Occludin was localized at the very apical compartment of the cell at the TJ region (Fig. 2-3A), and actin was distributed at the lateral and apical surface of the cell, forming thin filaments in the cytosol (Fig. 2-3B). Actin and occludin visually appeared

colocalized at the TJ region of the apical part of the cells (Fig. 2-3C). Following 6 h of incubation of *C. rodentium* with cell monolayers there was no change in occludin distribution (Fig. 2-3D), while there was some aggregation of actin beneath the apical cell surface (Fig. 2-3E, 2-3F). These changes increased dramatically over time. After12 h of incubation there was an increase in the amount of actin and occludin aggregation, which formed a punctate pattern beneath apical cell membrane (Fig. 2-3G, 2-3H, 2-3I). After 24 h of incubation normal actin and occludin structure was diminished and these proteins formed pedestals over the apical surface of the cells and in the TJ region (Fig. 2-3J, 2-3K, 2-3L). Occludin and actin pedestals appeared visually colocalized, with occludin distributed apically from actin (Fig. 2-3L).

C. rodentium alters gene expression in Ptk6 cells

Quantitative real time PCR analysis detected a 1.86 fold increase ($P < 0.1$) in transcription levels of *Cldn8* gene in *Ptk6* monolayers incubated with *C. rodentium* for 3 h. There was an unsignificant downregulation of *Cldn1*gene expression, while transcription of *Cldn5*, *Cldn7* was slightly upregulated in cells incubated with *C. rodentium.* The mRNA expression levels of *Gale4*, encoded for peptide involved in lateral cell adhesion and recognition of carbohydrates were up-regulated. There was downregulation of anion exchanger *Scl26a3* (*Dra*) in *C. rodentium* treated monolayers. The mRNA expression levels of *Kcnn4, Nkcc1, Aqp1, Adora2b, Itln1* and *Cnlp1* were insignificantly upregulated in response to *C. rodentium* treatment (Fig. 2-4).

Discussion

This study introduced novel *Ptk6* colonic epithelial cell line as a relevant model for studying *C. rodentium* infection as well as EPEC-induced-diarrhea *in vitro*. *C. rodentium*

interacts with *Ptk6* polarized monolayer in the mode, which closely resembled that seen in murine intestine inoculated with *C. rodentium* or EPEC (62, 83). *Ptk6* cell line can be used to study colonic epithelial cell response to A/E pathogens, and determine the key bacterial and host cell factors that determine the severity of the disease.

Intestinal barrier dysfunction induced by EPEC has been studied on various human (Caco-2, T84, HEK293) and animal cell lines (MDCK, CMT-93) (34, 107, 113). After discovering the genetic similarity between EPEC and murine enteric pathogen *C. rodentium* and the ability of *C. rodentium* to induce A/E lesions and diarrhea in mice, the *C. rodentium* infection in mice has been used widely as for an *in vivo* model for EPEC infections in humans (88, 97). However, the *in vivo C. rodentium* model and *in vitro* EPEC model possess some differences regarding intestinal epithelial cell response and pathogenic mechanisms of EPEC and *C. rodentium.* Furthermore it is difficult to study signaling pathways *in vivo* which necessitates the need for an *in vitro* model of *C. rodentium* infection that will allow investigation of the pathogenesis of this A/E pathogen as well as host response to the infection.

The murine rectal carcinoma cell line CMT-93 was established as *in vitro* model for *C. rodentium* infection (44), however, more research is needed to identify the similarities and differences between EPEC and *C. rodentium in vitro.* This study reports for the first time that *C. rodentium* induces pathophysiological responses in conditionally immortalized colonic epithelial *Ptk6* cells. Exposure of *Ptk6* cell monolayers to *C. rodentium* leads to decrease in R_{TE}, increase of paracellular permeability, actin pedestal formation, disruption of TJs, and changes in gene expression.

Attachment is the first step in A/E bacterial pathogenesis and is required to initiate host immune responses during EPEC infection (63, 73). Current study determined that *C. rodentium*

adheres to *Ptk6* cells shortly after inoculation, followed by increased attachment during later infection.

Epithelium in gastrointestinal (GI) tract serves as a barrier between luminal content and underlying tissues, which prevent luminal antigens from penetrating into submucosal layers. Colonic epithelium expresses various TJ proteins, including occludin, ZO-1 and claudins, which play important roles in maintaining epithelial integrity and R_{TE} (62, 117, 153). The initial characterization of murine *Ptk6* cells indicates formation of a resistant polarized monolayer (141). *Ptk6* cell line was used to examine the effect of *C. rodentium* on R_{TE} and epithelial permeability. Previous studies (9, 44) have shown that *C. rodentium* decreased R_{TE} of the cell monolayer and the permeability to large molecular weight compounds increased. In the normal colon, the paracellular resistance is approximately 23 times higher than transcellular resistance (58). Significant decreases in R_{TE} and increased flux of large solutes is consistent with disruption of the paracellular barrier rather than the transcellular, implying that TJs are important in maintaining the integrity of *Ptk6* monolayers. It has been recognized, that TJs are one of the main structures of epithelial barrier, and have an important role in some GI diseases, such as ulcerative colitis (117), Crohn's disease (152) and bacterial infections (62, 102, 121). Actin and TJ proteins, such as occludin, are affected by EPEC and *C. rodentium* (62, 87, 104, 153). This study has determined that *C. rodentium* induces actin polymerization and TJ protein occludin redistribution into pedestals on the apical surface of *Ptk6* epithelial cells. Occludin has been implied to regulate the epithelial permeability to large size molecules, without affecting R_{TE} (3). Thus, the increase of paracellular dextran flux in *Ptk6* cell culture model was most likely due to loss of normal occludin distribution, while decrease of *Ptk6* R_{TE} may be occludin-independent. The *C. rodentium*-induced decrease of R_{TE} may depend also on changes in the expression of

other components of TJs. *In vitro* studies on CMT-93 cells identified that *C. rodentium* disrupts claudin-4 and claudin-5 (44) and *in vivo* studies determined disruption of claudin-1, -3 and -5 following *C. rodentium* infection (62). Present study determined an increase in the mRNA levels of *Cldn8* gene, encoding for claudin-8, indicating the possible role of this TJ protein in maintenance of R_{TE}. Further studies are needed to determine the role of claudins in *C. rodentium* infection.

Previous studies of *C. rodentium* infection in C3H and FVB mice revealed that *C. rodentium* infection causes significant changes in the expression of genes involved in the epithelial ion transport and regulation. The SLC26A3 protein is involved in apical absorption of chloride by epithelial cells and secretion of bicarbonate into the lumen. The proteins NKCC1 and KCNN4 play a role in basolateral potassium absorption and secretion, respectively, and their expression is required for apical chloride secretion (11). It has been determined that *C. rodentium* infection causes downregulation of *Slc26a3* gene expression and an increase in expression *Kcnn4* or *Nkcc* genes in the epithelium of infected mice (20, 22). Although in this study significant changes in *Slc26a3, Kcnn4* or *Nkcc1* gene expression were not measured, there was observed an insignificant downregulation of *Slc26a3,* accompanied by increase in *Kcnn4* and *Nkcc1* gene expression. Thus, the present study expands on previous research revealing that *C. rodentium* may alter the expression of ion transporters providing a basic mechanism to study *C. rodentium* induced diarrhea *in vitro*.

Innate immunity is an important component of intestinal defense against pathogens. The cathelicidin-related antimicrobial peptide, encoded by *Cnlp* gene, has activity against A/E pathogens *in vivo* and *in vitro* (75, 149). An important component of host defense against bacterial infection, intelectin-1 (*Itln1*) serves as an intestinal lactoferrin-binding receptor in

mammals, competing for iron uptake with bacteria (126, 128). The increase in expression of genes encoding for these antibacterial proteins in *Ptk6* cells suggest a complex response of this cell culture model to murine pathogen *C. rodentium* and implies the importance of innate immune response during A/E infections.

This study reports the use of an *in vitro* model for *C. rodentium* infection, using the relevant conditionally immortalized murine colonic epithelial cell line *Ptk6.*The model is characterized by bacterial attachment, disruption of epithelial barrier function, and redistribution of actin and occludin following *C. rodentium* exposure. Gene expression analysis revealed that a number of genes encoded for epithelial ion transportrs and innate immunity were affected by *C. rodentium* infection in *Ptk6* cells. This study indicates the complex response of *Ptk6* cells to *C. rodentium* that results in change of monolayer morphology and physiology. The outcomes underscore the importance that TJs play in innate immunity and ion transport during *C. rodentium* pathogenesis *in vivo*. The closeness of *Ptk6* cell model to murine colonic epithelium is due to its unique ability to differentiate *in vitro* and the functional characteristics makes this cell line an ideal model to study *C. rodentium* infection.

Figures and Tables

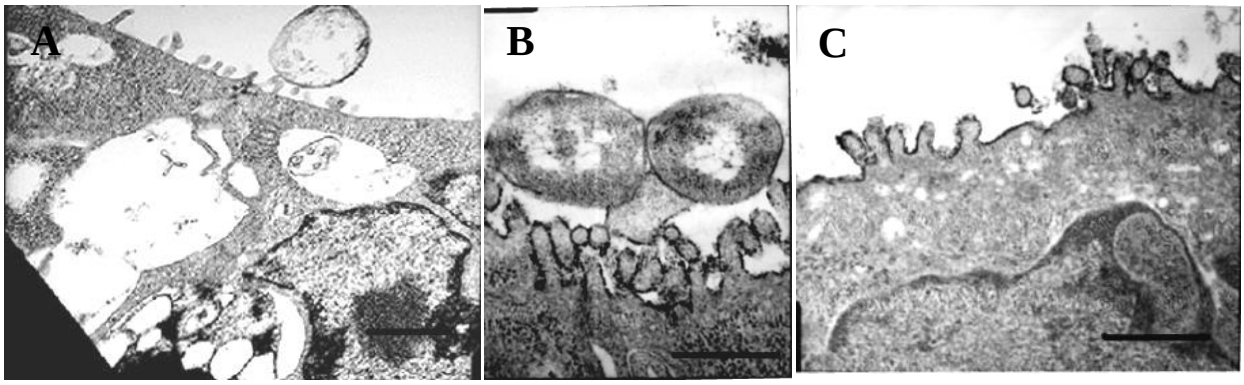

Figure 2-1 *C. rodentium* attached to *Ptk6* cells.

Transmission electron microscopy revealed that *C. rodentium* loosely attaches to the apical surface of *Ptk6* cells at 1 h after exposure (A). Bacterial attachment and pedestal formation on the apical surface of the cells following 12 h of incubation (B). Loss of microvilli and membrane ruffling on the apical surface following 12 h of exposure to *C. rodentium* (C). Bars represent 10 µm (B), 5 µm (C) and 20 µm (D).

Table 2-1 Genes involved in intestinal ion transport, innate antimicrobial activity, cell-cell connection and transcription regulation.

Gene	Primer name	Primer sequence	T_m	Main functions
Mouse GAPDH	*F49*	GGTGAAGGTCGGTGTGAACG/	48, 52 and	Glycolysis catalysist, reference gene in this study
	R281	CTCGCTCCTGGAAGATGGTG		
Potassium intermediate/small conductance calcium-activated channel, subfamily N, member 4	*Kcnn4 F*	TCTGCACGCTAGATGTTGT/	55°C	Potassium ion transport
	Kcnn4 R	GACAAAGGAGGAAGGCAGTG		
Solute carrier family 12, member 2	*Nkcc1F*	CGATGAGCTGGAAAAGGAAC/	55°C	Sodium:potassium: chloride cotransport
	Nkcc1R	TGTATGCGACCACAGCATCT		
Solute carrier family 15 (H+/peptide transporter), member 2	*Slc15a2 F*	GGATGACAGCCATCAGGTTT/	55°C	Oligopeptide and proton transport
	Slc15a2R	TCCTCTTTGCACAGTTCTGTACTC		
Adenosine A2b receptor	*Adora2b F*	TGCTCACACAGAGCTCCATC/	55°C	G-protein coupled receptor protein signaling pathway
	Adora2b R	GTGTCCCAGTGACCAAACCT		
Solute carrier family 26, member 3	*Slc26a3 F*	GGCAAAATGATCGAAGCCATAGG/	55°C	Anion exchanger activity, transport
	Slc26a3R	GATGGTCCAGGAATGTCTTGTGATGT		
Cldn 1 (Claudin1)	*Cldn1 F*	ACTGTGGATGTCCTGCGTTT/	55°C	Tight junctional protein
	Cldn1 R	CCAGCAGGATGCCAATTAC		
Cldn 5 (Claudin5)	*Cldn5 F*	CTGGACCACAACATCGTGAC/	55°C	Tight junctional protein
	Cldn5R	CAGATTCATACACCTTGCACTG		
Cldn7 (Claudin7)	*Cldn7 F*	CATGTACAAGGGGCTCTGGA/	55°C	Tight junctional protein
	Cldn7 R	GCTAAGAAGCCCAACACCAG		
Cldn 8 (Claudin8)	*Cldn8 F*	TGTCTGCCTTCATCGAAAGT/	55°C	Tight junctional protein
	Cldn8 R	GACCTTGCACTGCATTCTGA		
Aquaporin 1	*Aqp1 F*	AGCGAAATCAAGAAGAAGCTC/	48°C	Water transport
	Aqp1 R	CCTCTATTTGGCTTCATCTC		
Lectin, galactose binding, soluble 6	*Lgals6 F*	GTCCAACCTGTTGAAACCAA/	48°C	Carbohydrate recognition
	Lgals6 R	CCTATGTCCAGATCTGAGC		
Peroxisome proliferator-activated receptor gamma	*Ppar-γ F*	TTGCTGAACGTGAAGCCCATCGAGG/	48°C	Regulation of fatty acid storage and glucose metabolism
	Ppar-γ R	GTCCTTGTAGATCTCCTGGAGCAG		
Nucleolin NH2	*Ncl F*	ATGGTGAARCTCGCAAAGGCHG/	48°C	Synthesis and maturation of ribosomes
	NclR	CAAAACCCACGGAGAGTC		
Intelectin	*Itln-1 F*	ATG ACC CAA CTG GGA TTC CTG/	52°C	Carbohydrate recognition
	Itln-1 R	TCA GCG ATA AAA CAG AAG CAC G		
mCRAMP	*Cnlp R*	CTTCAACCAGCAGTCCCTAGACA/	52°C	Cathelicidin-related antimicrobial peptide
	Cmlp R	TCCAGGTCCAGGAGACGGTA		
Galectin-4	*Gale4F3*	CAACCCTCCACAGATGAACACCTT/	52°C	Carbohydrate recognition
	Gale4R2	TCCAGCGTGTCTACCATTTGGAAT		
FBJ osteosarcoma oncogene B	*Fosb F*	TTCCTAGTGACACCTGAGAGCTG/	52°C	Regulation of transcription
	Fosb R	GAACATTGACGCTGAAGGACTAC		

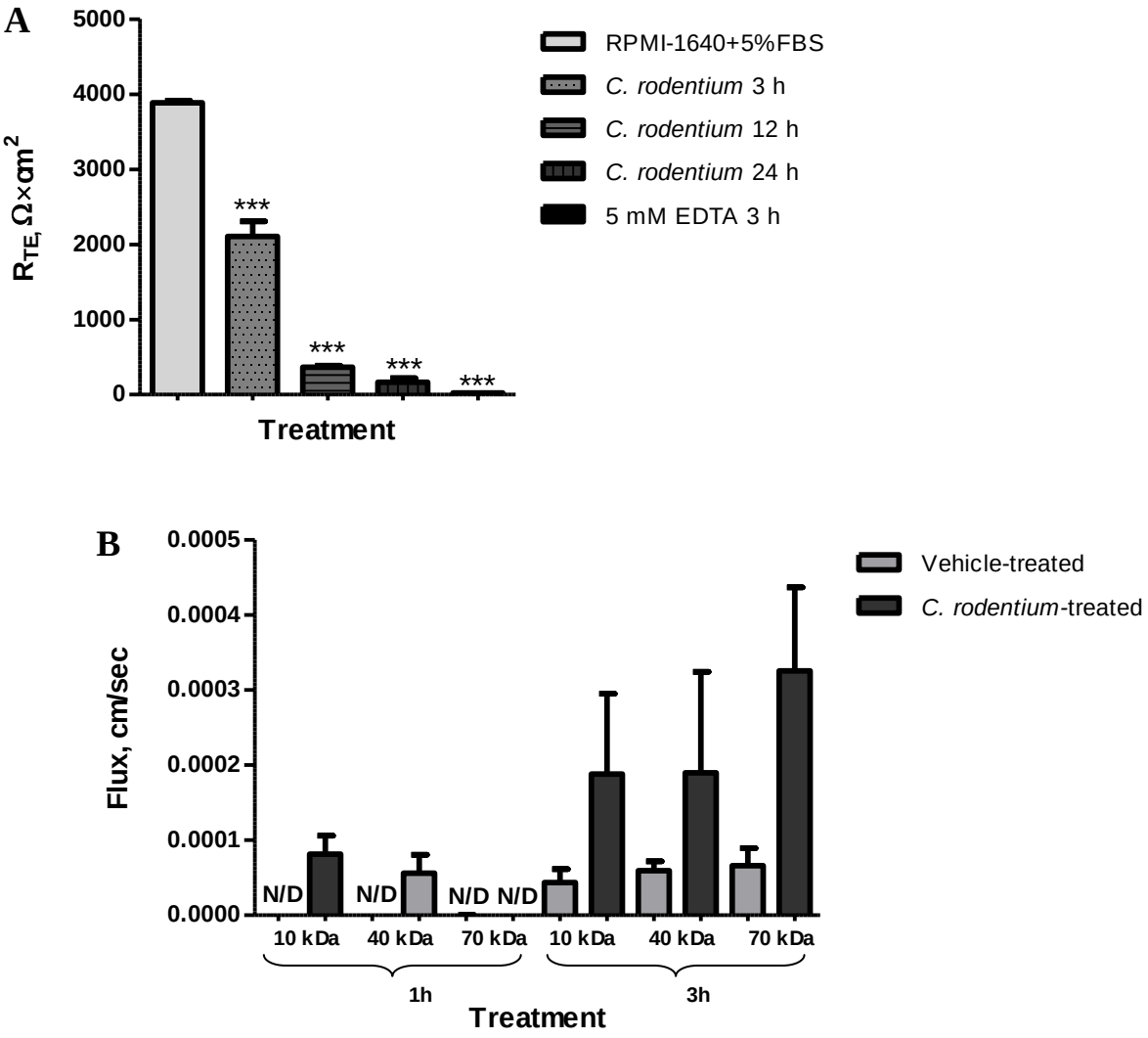

Figure 2-2 Exposure *Ptk6* monolayers to *C. rodentium* resulted in loss of integrity barrier and increase of epithelial permeability to high molecular weight molecules.

Exposure to *C. rodentium* for 3 h significantly decreased R_{TE} of *Ptk6* monolayers compared to cells treated with RPMI-1640 only (A). Cell monolayers became more permeable to 10 kDa and 40 kDa dextrans after 1 h of exposure, while permeability to 70kDa dextran increased after 3 h of incubation with *C. rodentium* (B).

***, P <0.0001. N/D – not determined.

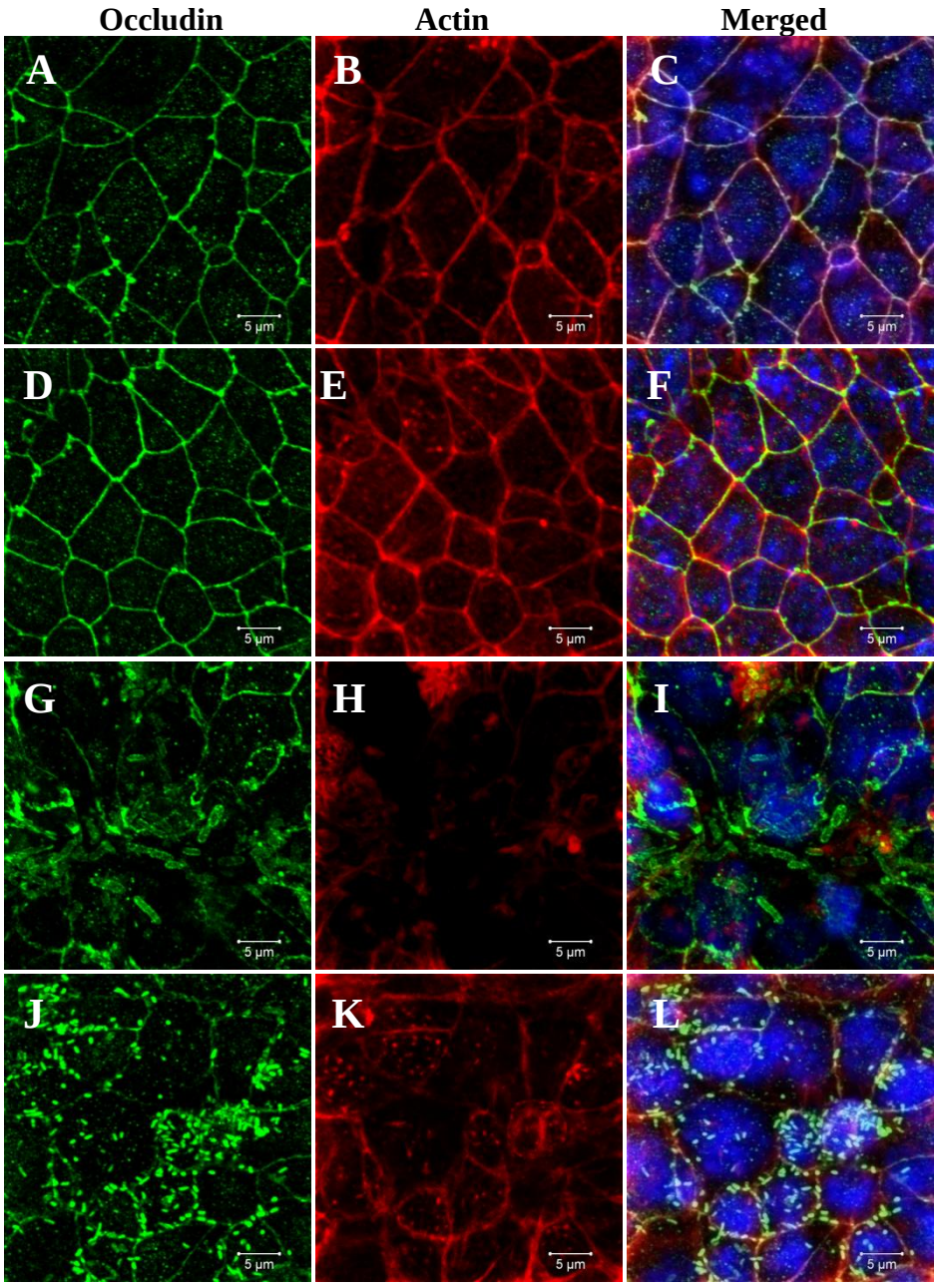

Figure 2-3 Tight junctional proteins relocalized upon exposure to *C. rodentium*.

Distribution of occludin (green) and actin (red) in *C. rodentium*-untereated *Ptk6* monolayer (A, B). Normal occludin distribution and actin pedestal formation 6h after exposure to *C. rodentium* (E, D). Actin and occluding pedestals following 12 h exposure to *C. rodentium* (G, H). Punctate distribution of actin and occludin 24 h after incubation (J, K). Merged pictures of control and *C. rodentium*-treated monolayers (6 h, 12 h and 24 h) respectively (C, F, I, L). Nuclei are stained in blue.

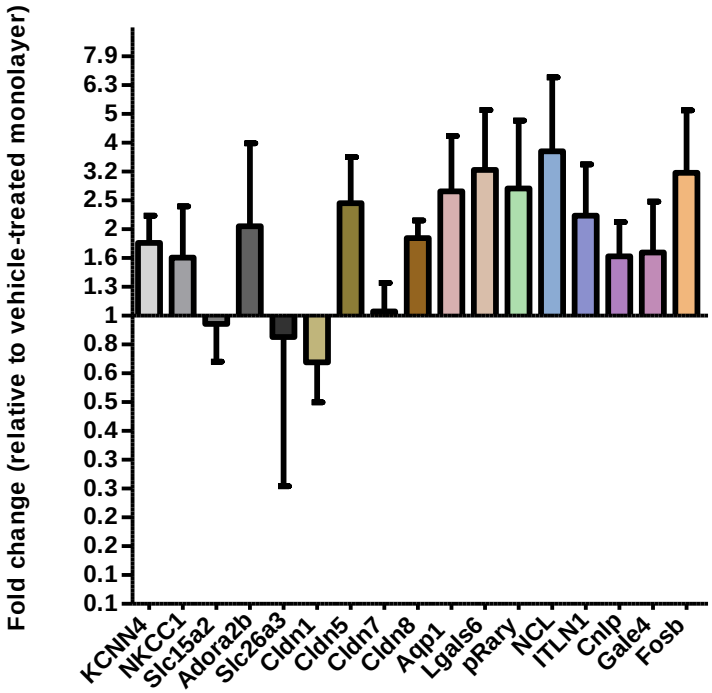

Figure 2-4 Exposure of cell monolayers to *C. rodentium* for 3 h induced upregulation of *Cldn8* gene.

There was upregulation ($P < 0.1$) of *Cldn8* while the expression of other genes at mRNA level was not significantly affected by *C. rodentium*. The expression of genes was normalized to that of RPMI-1640 only-treated monolayer.

Chapter 3 - *C. rodentium* induces morphological and physiological changes in colonic epithelium of C3H and SW mice

Abstract

Citrobacter rodentium causes transmissible murine colonic hyperplasia and is used as a model for enteropathogenic and enterohemorrhagic *Escherichia coli* infections. While *C. rodentium* causes little mortality in most mice, some strains, such as C3H mice, develop fatal colitis. The objective of this study was to compare structural and functional changes in the colonic epithelium of adolescent (5-week old) Swiss Webster (SW) outbred and C3H inbred mice following intracecal inoculation with *C. rodentium.* Colons, livers, spleens and mesenteric lymph nodes of C3H mice had higher bacterial loads than SW mice. Tight junction disruption and pedestal formation were observed in the colonic epithelium of both strains. Occludin and actin pedestals were located subjacent to the attached bacteria. Occludin and actin aggregations were more evident, and located throughout the epithelial surface in inoculated C3H mice. There was a significant increase in transepithelial electrical resistance in colons of inoculated C3H mice. The gene expression assay determined significant transcriptional changes in the expression of genes involved in the ion transport and its regulation (*Slc26a3*, *Nkcc1* and *Adora2B*) as well as innate immunity regulators such as *Cnlp* in the colon of C3H mice. The expression of gene encoding tight junctional protein claudin-5 was higher in inoculated C3H mice. These results support the hypothesis that *C. rodentium* infection in mice may be associated with fluid loss due to impaired chloride absorption. A decrease in innate immune response may be partially responsible for more severe disease in C3H mice. Various changes in the colonic epithelial structure and dynamics of susceptible and resistant strains of mice indicate the role of the host in the disease. This study identified the host factors that play an important role in the *C. rodenitum*-

induces infection, and may further be targeted in the development of preventive care and treatment of infectious diarrhea.

Introduction

Acute diarrhea is one of the most important illnesses in humans, especially in children under age of five in developing countries. Attaching and effacing (A/E) pathogens such as enteropathogenic (EPEC) and enterohemorrhagic (EHEC) *E. coli* common causes of acute bacterial diarrhea.Mice do not develop overt disease or pathology in response to *E. coli* infection, and are able to clear out the pathogen in 14-28 days post-inoculation (dpi) with minimal clinical signs or lesions. These associations are opposite to those seen after inoculations with *C. rodentium*, where mice readily develop transmissible colonic hyperplasia and A/E lesions (83, 97). *C. rodentium* (formerly *C. freundii* biotype 4280) contains DNA homologous to effacing and attaching gene (*eae*), which is necessary for A/E activity of pathogenic *E. coli* (115, 116). The pathogenic properties of *C. rodentium* along with the availability of novel reagents suggest that this bacterium is a part of appropriate murine model for *E. coli* infection of humans. The disease outcome depends on several factors such as diet and age, but is not influenced by gender. The disease results in high mortality in young and suckling animals, while adult mice often survive (89). Clinical signs of *C. rodentium* infection in mice are nonspecific and include ruffled coat, weight loss, depression, stunting, perianal fecal staining, pasty dark feces and dehydration (98). Dietary interventions do not alter the time course of *Citrobacter* infection (129), while dosing of mice with probiotics prior to *C. rodentium* inoculation significantly decreased infection and enteropathy (27, 33, 79). Susceptibility to *C. rodentium* also depends on the genetic background of the mice. Germfree CF1 and C3H mice are highly susceptible to infection while

germ-free C57BL/6 and NC mice are moderately susceptible, and germ-free BALB/c are resistant (77). Mice lacking alpha chain of cluster of differentiation 8($CD8\alpha^{-/-}$) and mice deficient in delta chain of T cell receptor ($TCR\text{-}\delta^{-/-}$) were able to resolve *C. rodentium* infection due to production of T-cell dependent serum antibody, while $CD4^{-/-}$ and $TCR\text{-}\beta^{-/-}$ mice develop polymicrobial sepsis and end-organ damage (abscesses) resulting in high mortality during acute infection (25). Adult mice of many strains, including Swiss Webster (SW), develop self-limiting epithelial hyperplasia when infected, whereas adult C3H and FVB mice are highly susceptible to infection and demonstrate 60-100% mortality rates two weeks after infection (21, 22). Susceptible strains of mice also have higher bacterial translocation to mesenteric lymph nodes (22, 130). Hypovolemia could be the cause of death in FVB and C3H mice. Severe dehydration could be due to increase in paracellular permeability, as well as dysregulation of apical and basolateral ion channels (20, 22). *C. rodentium* interacts with actin cytoskeleton and tight junctions (TJs), and initiates host immune response (9, 25, 131). Recent study (20) identified that substantial fractions of genes involved in intestinal epithelial ion transport and its regulation were affected upon *C. rodentium* infection. It was suggested that intestinal ion disturbances rather than immune related processes are responsible for severe diarrhea in susceptible strains of mice (20). One of the major proteins involved in intestinal chloride loss was SLC26A3 (DRA), which was down-regulated in susceptible mice (22).

In spite of more than a decade of research, the mechanisms of *C. rodentium* infection and the changes that occur in the intestine of various strains of mice are not completely understood. The objective of this study was to evaluate both morphological and physiological changes that occur in the colonic epithelia of young susceptible C3H and relatively resistant SW mice following direct intracecal inoculation with *C. rodentium.*

Materials and methods

Mice strains

Female inbred C3H/HeOuJ (TLR4 sufficient and endotoxin sensitive) (20 mice), and outbred Swiss Webster Tac:SW (20 mice) mice were purchased from Taconic Laboratories and Jackson Laboratory (Bar Harbor, ME and Germantown, NY, USA respectively) at 4 weeks of age. Mixing of bedding until the time of inoculation (five weeks of age) was performed to obtain comparable microbial status and minimize commensal microbiota biases. Animals were housed in microisolator cages in a pathogen-free facility and maintained on pelleted rodent chow and water, *ad libitum*.

All procedures involving animals were approved by the Institutional Animal Care and Use Committee of Kansas State University (IACUC# 2805.4).

Bacterial strains and infection of mice

Bacteria were grown overnight in Luria-Bertani (LB) broth at 37°C with shaking, diluted 1:10 with Luria broth, and incubated until OD_{600} reached 0.6 (approximately 2×10^8 CFU/ml). Ten ml of the culture was centrifuged at 3,000 rpm for five min and the resulting pellet resuspended in an equal volume of phosphate buffered saline (PBS: 137 mM NaCl, 2.7 mM KCl, 4.3 mM Na_2HPO_4, 1.47 mM KH_2PO_4, pH 7.4).

At five weeks of age, mice were assigned randomly to control (mock infected: five mice) or infected (15 mice) groups. Prior to surgery and following inoculation, mice were anesthetized (ketamine 100 mg/kg and xylazine 10 mg/kg given intraperitoneally). In addition, isoflurane gas was applied via a face mask at 1-3% for maintenance of anesthesia, when necessary. Mice were

inoculated with wild type *C. rodentium* DBS120 (kindly provided by Arek Raczynski, Massachusetts Institute of Technology) via intracecal injection.

Mice were inoculated by direct injection of bacterial culture into the base of cecum. A midline laparotomy was performed with injection 50 μL containing 1×10^7 CFU of *C. rodentium* (infected) or PBS (control), directly into the base of the cecum. Following the injection, as the needle was withdrawn from the cecum, a cotton swab was placed over the injection site to absorb any leakage. A second swab was then placed over the injection site to confirm the cessation of leakage. The incision site was closed as a double layer: the abdominal muscle layer was closed using an absorbable suture and the skin layer was closed with wound clips. Animals were monitored twice daily and when any mouse showed signs of severe discomfort or outward morbidity, it was euthanized humanely.

Sample collection

C3H mice were euthanized 2, 4, 7, 8, and 10 dpi; SW mice were euthanized 2, 4, 7, 10, and 14 dpi. Animals were euthanized individually in a CO_2 chamber, followed by cervical dislocation. Whole colon was removed aseptically and samples were collected. Tissues from the border of proximal and distal colon were used for bacterial enumeration. Feces from that area were collected for bacterial shedding enumeration. Proximal pieces of colon were saved in cold Ringer solution (120 mM NaCl, 25 mM $NaHCO_3$, 3.3 mM KH_2PO_4, 0.8 mM K2HPO_4, 1.2 mM $MgCl_2$, and 1.2 mM $CaCl_2$) containing indometacin (50 μM, Sigma-Aldrich, Saint Louis, MO) for further transepithelial electrical resistance (R_{TE}) assay. Distal colon samples were fixed in 4% buffered paraformaldehyde (Fisher Scientific International, Hampton, NH), and then frozen on dry ice in Optimal Cutting Temperature (OCT) media (Tissue-Tek, Sakura Finetek Europe B.V., The Netherlands), and stored at -80°C for immunocytochemistry. For histology distal colon

samples were incubated in Karnovsky's fixative overnight. Distal colon tissues were cut into small pieces and stored in RNA later (Ambion, Inc, Carlsbad, CA) at -80^{0}C for further RNA extraction. Mesenteric lymph nodes (MLN), liver and spleen were isolated and placed in LB broth containing 50 µg/ml of kanamycin (Sigma-Aldrich).

Bacterial enumeration

Colonic tissues, fecal pellets, lymph nodes, liver and spleen were homogenized (4710 Ultrasonic homogenizer, Cole Parmer Instruments), serially diluted and plated onto LB agar with kanamycin (50 µg/ml) for selective growth of *C. rodentium*. Bacterial colonies were enumerated the following day. *C. rodentium* formed small to medium circular, convex, off-white colonies that allowed distinguishing them from contamination.

Histopathological evaluation, immunocytochemistry and confocal imaging

Paraffin-embedded colonic tissue sections (4 µm) stained with hematoxylin and eosin (Histo Lab, Kansas State University) are examined. Digital pictures were acquired with light microscope (Nikon Eclipse 600, NY).

Frozen tissues embedded in OCT media were sectioned at 14 µm (CM3050S, Leica,Germany) and dried in slide warmer (Fisher Scientific) for 3 h. Cryosections were permeabilized in 0.5% TritonX for 30 min, incubated overnight in blocking solution (PBS containing 5% BSA and 0.1% Tween 20). Slides were incubated overnight with primary antibodies (Rabbit anti-occludin, Invitrogen, Carlsbad, CA) diluted in blocking solution at a concentration of 5 µg/ml. Secondary antibodies (10 µg/ml, Goat anti rabbit, Invitrogen), diluted in blocking solution, were applied for 2 h. Actin and nuclei were visualized by staining with Alexa fluor phalloidin and DAPI (Invitrogen), respectively, for 40 min. Following staining,

sections were mounted in FluorSave reagent (Calbiochem, La Jolla, CA) and covered with cover slips. To assess the specificity of labeling, tissues and bacterial cultures were labeled with secondary antibodies only, which resulted in a lack of immunofluorescence (data not shown).

Cryosections were viewed by laser-scanning microscopy using similar intensities of red (555 nm), green (488 nm), and blue (405 nm) laser lights (LSM 700, Carl Zeiss, Göttingen, Germany). Transmitted light intensities were recorded and color images were generated by addition of red, green, and blue images. For each experiment, 8-12 images of planes at various depths within the sample (z stacks) were acquired. Each z stack integrated 60-90 images with the resolution 1024×1024 pixels. Virtually superimposed images were obtained using software provided with the confocal laser scanning microscope (Zen 700, Carl Zeiss). Observations reported are based on at least three independent observations.

Gene expression studies

RNA was extracted from colon samples using TRIzol Reagent. Briefly, 1 ml of TRIzol Reagent (Invitrogen) was added to each sample and incubated for five min at room temperature. Then, chloroform (200 µl) was added, mixture was shaken several times, and centrifuged for 15 min at 12,000 rpm. The clear upper phase was transferred to a new tube, mixed with 500 µl of ice cold isopropanol, incubated for 10 min at room temperature, and centrifuged for 10 min at 12,000 rpm. The resulting pellet was washed with 75% ice cold ethanol, and resuspended in 50 µl of distilled nuclease free water. The DNase I (amplification grade, Invitrogen) was added to eliminate any DNA in the sample. Quantitative RT-PCR was performed using SuperScript III Platinum SYBR green One-Step qRT-PCR kit (Invitrogen) on a Thermocycler (RealPlex machine, Eppendorf, Hauppauge, NY). Reverse transcription was completed for 30 mins at 50°C followed by one min of denaturation at 95°C. PCR amplification was continued for 40 cycles:

94°C for 15 sec (denaturation), 48-55°C for 30 sec (annealing) and 72°C for 30 sec (extension). The gene expression study was carried at the mRNA level, where the changes in levels of expression for protein coding genes were compared. The mRNA expression profiles of C3H and SW mice were calculated as fold-changes using $\Delta\Delta C_t$ method. Target genes for qRT-PCR analysis, and annealing temperatures are listed in Table 1.

Transepithelial electrical resistance measurement

Transepithelial electrical resistance was measured in modified Ussing flux chambers (VCC MC8, Physiological Instruments, San Diego, CA). Colons were opened along their mesenteric borders, and cleaned with cold (4ºC) Ringer solution containing indomethacin. Tissues were mounted in modified Ussing chambers and bathed in Ringer's solution containing 10 mM glucose bubbled with 5% CO_2 and 95% O_2. Voltage and current measurements were acquired and calculated as described (93). To test various experimental hypotheses, monolayers were exposed to amiloride (10 µM), bumetanide (20 µM), 1-ethyl-2-benzimidazolinone (EBIO-300 µM) and forskolin (2 µM) (Sigma-Aldrich) as described (124).

Data analysis

All statistical analyses were performed using the statistical software GraphPad Prism version 5.00 for Windows (GraphPad Sofrware, San Diego, CA) or SAS version 9.2, (SAS, Cary, NC). Data were presented as means ± SEM, and the level of significance for all tests was set at $P < 0.05$. Colony counts were $\log_{10}$ transformed, and means and SEs of the mean were calculated from the $\log_{10}$ values. The R_{TE} values were averaged for days 2-7. Group comparisons were made by analysis of variance, followed by Tukey's test. An analysis of variance, followed

by an unpaired t-test was performed to compare mean differences in gene expression levels between C3H and SW mice

Results

C. rodentium induces severe disease in C3H mice, but not in SW mice

C3H mice inoculated with *C. rodentium* were extremely susceptible to the bacteria and developed disease leading to 100% mortality by 8 dpi. SW mice developed mild clinical signs and survived throughout 14 days of study. Bacterial shedding was higher in C3H mice than in SW mice, but did not depend on the day of study (Fig. 3-1A). Bacterial loads in the colon were consistently higher in C3H mice up to 7 dpi. Colonic bacterial counts increased more slowly in SW mice, which were consistent with lower fecal levels immediately following inoculation (Fig. 3-1B). This study revealed that low numbers of bacteria were translocated to mesenteric lymph nodes (MLN), liver and spleen of infected mice (Fig. 3-1C, 1D and 3-1E). Bacterial numbers recovered from MLN and liver of C3H mice were higher than SW mice (Fig. 3-1C and 3-1D). Bacteria were undetectable in spleen of SW mice at 2 and 4 dpi, but were comparable to C3H mice at 7 dpi (Fig. 3-1E).

Colonic changes in C3H and SW mice inoculated with C. rodentium

Histological changes were consistent with the rates and degree of bacterial colonization in C3H and SW mouse strains. In C3H mice, colons were thickened and rigid by four dpi, with fluid and mucus accumulation in the lumen (visual examination, data not shown). In contrast, colons of SW mice were filled with well-formed stool pellets, and visible changes in morphology were observed only at 10 dpi (data not shown). In both mouse strains at 2 dpi, bacteria were

localized superficially, with higher bacterial loads in C3H mice (Fig. 3-2A and 3-2B). At 7 dpi, *C. rodentium* loads were extremely high in the lumen and crypts (Fig. 3-2C), and were even observed in muscularis mucosa of C3H mice (Fig. 3-2E). Hyperplasia was more prominent in C3H mice, resulting in loss of crypt morphology, high inflammatory cell infiltration of epithelium, hemorrhages and ulceration at 7 dpi (Fig. 3-2C). In SW mice, the bacteria were localized primarily on the luminal surface of the epithelia, and the colon had well preserved tissue morphology with mild hyperplasia and insignificant inflammatory cell infiltration (Fig. 3-2B and 3-2D).

C. rodentium induces increase in transepithelial electrical resistance in the colon of C3H mice

A physiological barrier separates the lumen from underlying tissues and is important for the normal function of the colon. The epithelial monolayer contributes most to the colonic resistance and gut barrier function. Subepithelial connective, nervous, and muscular tissues do not significantly contribute to the barrier function. Hence, the transepithelial barrier is measured as overall transmural resistance (58). In the present study transepithelial electrical resistance was measured to determine the epithelial integrity after exposure to PBS or *C. rodentium*. To identify the changes in the functioning of the epithelial ion channels and transporters, series of treatments were used: amiloride to block Na^+ reabsorption via the epithelial Na^+ channel ENaC; 1-ethyl-2-benzimidazolinone (EBIO), which activates Ca^+ sensitive K^+ channels (51); forskolin to increase cytosolic generation of cAMP, which induces anion secretion; and bumetanide to block the basolateral cotransporter, NKCC1, which contributes to anion loading for secretion.

This study determined an interesting pattern: the R_{TE} of the colon of C3H mice inoculated with *C. rodentium* was consistently higher (P <0.0001) than these of vehicle-inoculated C3H

mice, independently of applied treatment. The colonic R_{TE} of SW mice did not change significantly after *C. rodentium* inoculation. Overall, the drug treatment did not seem to affect R_{TE} in inoculated and control mice of both strains. The R_{TE} of the colon of *C. rodentium*-inoculated C3H mice was significantly higher (P <0.0001) than that of *C.rodentium*-inoculated SW mice, but there were no significant differences in R_{TE} between vehicle-inoculated mice of both strains (Fig. 3-3).

No significant difference in colonic short circuit current (I_{SC}) was observed between C3H and SW mice and no significant difference was found between the *C. rodentium*-inoculated and vehicle-inoculated mice (data not shown). The short-circuit current was lower in the colon of *C. rodentium*-inoculated C3H mice compared to vehicle-inoculated at 4 dpi, while there was no difference observed in SW mice. In C3H mice, the I_{SC} was diminished at the basal state (in the absence of added amiloride, forskolin, EBIO and bumetanide), as well as after adding exogenous substances (Fig. 3-4A, 3-4B).

C. rodentium causes more prominent actin and occludin rearrangement in epithelium of C3H mice

In the colonic epithelia of vehicle-inoculated mice, occludin was primarily localized in the TJ region, forming reticular pattern at the apical border of the epithelial cells (Fig. 3-5A). Actin was distributed in the brush border (BB) and along the lateral cell margins in the colonic epithelium (Fig. 3-5B). In vehicle-inoculated mice, actin and occludin were colocalized at TJs, as indicated on the virtually superimposed picture (Fig. 3-5C). In *C. rodentium*-inoculated mice, occludin was relocalized from TJs to the apical cell membrane, forming punctate attern (Fig. 3-5D). *C. rodentium* inoculation induced actin cytoskeleton rearrangement and formation of actin-

rich pedestals (Fig. 3-5E). Actin pedetals were associated with occludin aggregations, where occludin was often located at the top of actin pedestal, or laterally from it (Fig. 3-5F).

In accordance to histological changes, the speed and degree of occludin and actin relocalization was higher in C3H mice than in SW mice. In C3H mice, changes in occludin and actin distribution were observed as early as 2 dpi (Fig. 3-5G), compared to lack of visible changes in SW mice (Fig. 3-5H). At 4 dpi, changes in occludin and actin localization were detected in SW mice (Fig. 3-5J), but these changes were more obvious in C3H mice (Fig. 3-5I). While in C3H mice actin and occludin pedestals formation increased in the surface epithelia and spread throughout the crypt by 7 dpi (Fig. 3-5K). These changes were less apparent in SW mice, with little or no pedestal formation in the lower crypt (Fig. 3-5L).

C. rodentium alters gene expression in murine colonic epithelium

Although non-significant, there were differences in gene transcription levels of mucosal lactoferrin *Itln1*, murine cathelicidin-related peptide *Cnlp,* lectin galactoside-binding protein *Gale4* and transcription promoter *FosB* between C3H and SW mice at 2 dpi. While levels of expression of *Cnlp* and *Itln1* were decreased in C3H mice compared to SW, *Gale4* and *Fosb* were increased (Fig. 3-6A). At 4 dpi *C. rodentium* inoculated C3H mice demonstrated increased expression levels of *Nkcc1* compared to SW mice (P <0.05). *C. rodentium* infection caused decrease in expression levels of mRNA encoded for adenosine receptor *Adora2b, Slc26a3 (Dra)* and TJ protein *claudin-5* in both mouse strains compared to control mice. However, levels of expression of *Adora2b* (P <0.01) and *claudin-5* genes were higher in C3H than in SW mice, while levels of expression of *Slc26a3* were decreased in C3H mice compared to SW (P <0.05) (Fig. 3-6B). To further validate these observations we analyzed the expression of genes in colonic tissues at 7 dpi. The transcription levels of *Nkcc1*, *Adora2b,* and peroxisome proliferator

activated receptor γ *pParγ* were decreased in C3H mice, compared to SW mice (P <0.05). Consistent with observations from 2 dpi, the mRNA levels of *Cnlp* were decreased in C3H mice (P <0.05) (Fig. 3-6C).

Discussion

Due to ability of *C. rodentium* to induce hyperplasia in the distal colon of mice, this murine pathogen has been used to study human diseases with predisposition to colorectal cancer, such as inflammatory bowel disease (IBD) (71). In the colon of infected mice *C. rodentium* produces characteristic to EPEC A/E lesions that feature pedestal formation and loss of microvilli on the apical surface of the colonic epithelial cell, but causes more severe disease in mice than EPEC (97) Hence, *C. rodentium* infection in mice is widely used as an animal model for EPEC infection, allowing investigation of bacterial virulence mechanisms, as well as host defense factors that play role in the disease (88, 114).

The aim of this study was to determine morphological and physiological changes in the colonic epithelium of *C. rodentium*-inoculated mice. This study revealed the differences in host epithelial response of highly susceptible C3H and relatively resistant SW mice to murine A/E pathogen *C. rodentium.* This study reports that C3H mice exhibit higher bacterial loads, more severe colonic lesions, disorganized TJs and altered gene expression, and overall develop more severe disease than SW mice.

Confirming previous work (9, 22, 25, 130), this study determined that C3H mice had higher bacterial loads in the colon compared to SW mice, while small numbers of *C. rodentium* were internalized into colonic epithelium and were able to colonize MLN, liver and spleen of both mouse strains. The intestinal lesions, including hemorrhage, ulcers, and inflammatory cell

infiltration were more obvious in C3H mice as well. The delayed increase in number of bacteria isolated from distant organs of SW mice was consistent with delayed increase of bacterial numbers isolated from feces and colon, indicating slower infection progression in SW mice.

Epithelial TJs form a continuous barrier at the boundary between the apical and basolateral membrane domains. In the intestine TJs separate internal and external compartments of the gut and regulate selective movement of solutes across the epithelium (42, 59). *C. rodentium* along with other A/E pathogens such as EPEC, EHEC and rabbit EPEC (REPEC) forms A/E lesions characterized by recruitment of F-actin and TJ proteins to sites of bacterial attachment, resulting in formation of actin-rich pedestals (32, 73, 104). Supporting these data, the current study showed that *C. rodentium* induced actin polymerization in colonic epithelial cells of C3H and SW mice, accompanied by formation of occludin aggregations on the top or laterally from actin-rich pedestals. Actin/occludin pedestal formation was consistent with speed of bacterial colonization, being evident first in C3H mice. In C3H mice actin and occludin aggregations were formed over the whole surface of epithelium and crypts, while in SW mice these aggregations were predominantly formed at the surface epithelia, with lesser extent in crypts. Remembering that pedestal formation requires direct bacterial attachment (63), and considering less intense pedestal formation in the colon of SW mice, it can be hypothesized that these mice have preventive mechanisms, which allow them to reduce bacterial attachment, especially in crypts.

C. rodentium induces marked decrease of R_{TE} in *in vitro* cell cultures (9, 44) and loss of epithelial barrier function in the colons of infected mice (62), besides disrupting TJs. Unexpectedly, in this study was observed an increase in colonic R_{TE} of inoculated C3H mice. This suggests that observed increase in R_{TE} could be due to change of certain TJ proteins

expression and /or due to increase in area occupied by TJs. In the epithelium, as in any 3D system, R_{TE} and solute flux partially depend on cell geometry. *C. rodentium* leads to severe epithelial hyperplasia in colon, increasing the number of cell per crypt 2-3 times more than in normal tissue (89). It is known, that R_{TE} in crypts is 3 times higher than in surface epithelia (58). Thus, the increase in numbers of cells that possess TJs, and form highly resistant epithelia may be the reason for increase in R_{TE} in the colon of inoculated C3H mice. We hypothesize that the increase in R_{TE} could also be partially due to the change in expression of claudins in colonic epithelial cells of *C. rodentium*-inoculated mice. Supporting this hypothesis, we observed an increase in expression levels of *Cldn5* in *C. rodentium*-inoculated C3H mice compared to SW. Previous studies have also demonstrated the role of claudin-5 in increased barrier function and paracellular sealing (4, 43).

Remarkable occludin redistribution in colonic epithelium was observed in this study. However, it was not clear until recently whether occludin is functionally important in maintaining epithelial barrier integrity (148). It has been determined that occludin forms a selective semi-permeable pore to large molecular weight molecules without contributing to R_{TE} (3). Hence the increased R_{TE} in C3H colonic epithelium observed in our study is likely to be occludin-independent. However, occludin disruption may contribute to higher bacterial translocation into the liver of *C. rodentium*-inoculated C3H mice.

Diarrhea and subsequent dehydration are the hallmarks of *C. rodentium* infection in mice. Initially, increased ionic secretion was suspected as a causative factor of colitis-associated diarrhea. In fact most inflammatory mediators, such as prostaglandins, platelet-activating factor, histamine, TNF and IL-1 have secretory effects *in vitro*. However, colonic epithelial Cl^- absorption was decreased during EPEC infection (57), and that when combined with increased

Cl^- secretion, may induce diarrhea. Studies conducted by Borenshtein *et al.* (20) revealed that susceptible FVB mice possessed profound downregulation of majority of apical transporters involved in Na^+ and Cl^- absorption, along with upregulation of basolateral transporters, providing the driving force for chloride secretion. There were also observed increased chloride levels in feces of susceptible C3H and FVB mice accompanied by hypochlorinemia (20, 22). In this study we determined that levels of *Slc26a3* were diminished in C3H mice accompanied by upregulation of expression of *Nkcc1* and *Adora2b* genes, which may indirectly suggest decreased absorption and increased secretion of chloride in colonic epithelium of C3H mice. Studies performed on inflamed colon *in vivo,* determined that colonic I_{SC} was diminished compared to non-inflamed specimens (94), suggesting that diarrhea may not be solely caused by excessive ionic secretion. We observed a reduced I_{SC} response in colonic tissues from *C. rodentium*-treated mice compared to vehicle-treated C3H mice. The observed diminished response to amiloride may be due to attenuated sodium channels; decreased effect of forskolin and EBIO may be due to *C. rodentium*-induced upregulation of potassium channels and CFTR. This study we provide evidence that *C. rodentium*-induced diarrhea partially occurs due to decreased absorption and increased secretion of chloride.

The innate immune response has a significant role in the development of *C. rodentium* induced diarrhea, by maintaining gut homeostasis, and interfering bacterial colonization. It was discovered that murine cathelicidin-related antimicrobial peptide, mCRAMP, encoded by *Cnlp* gene, is produced primarily by colon surface epithelial cells has antimicrobial activity against *C. rodentium,* and decreases bacterial colonization in mouse colon at early stage of the infection (75). In this study, the transcript levels for the *Cnlp* gene were reduced in C3H mice, compared to increased levels in SW, which may contribute to lesser colonization of this strain and reduced

colonic inflammation. Interestingly, the transcript levels of *Itln1* insignificantly increased in SW mice shortly after inoculation, implying important role of innate immune system in defense against *C. rodentium*.

In conclusion, this study demonstrates that *C. rodentium* induces colonic lesions, disrupts the epithelial barrier and alters the colonic epithelial gene expression differentially between C3H and SW mice. This study provides information about changes in the colon epithelium which occurs in the host in response to *C. rodentium* and emphasizes the importance of host factors in the disease progression in susceptible and resistant strains of mice. Disruption of TJs and A/E lesion formation has been implied as an important factor in *C. rodentium* pathogenicity. Additionally, this study suggests that multiple processes in colonic epithelium contribute to disease outcome. Lesser degrees of pathological changes in SW mice may be due to increased activity of innate immune defense proteins such as mCRAMP and ITLN1.Consistent with previous studies (22), this work suggests that *C. rodentium*-induced diarrhea in C3H mice may be caused partially by impaired chloride absorption as a potential result of profound downregulation of *Slc26a3*. This study for the first time reports the increase in colonic R_{TE} in *C. rodentium*-inoculated C3H mice. Although this result is inconsistent with previous reports (9, 44), the observed increase in R_{TE} may result from more complex responses to infection in colon than in cell-culture model. However, the underlying mechanisms of this change in epithelial barrier function require further investigation. Coordinated changes, such as an increased inflammation, hyperplasia, reorganization of cytoskeletal and TJ proteins, and changes in gene expression observed in susceptible C3H mice may provide a basic mechanism for the development of *C. rodentium* induced diarrhea in susceptible strains compared to relatively resistant strains of mice.

Table 3-1 Genes involved in intestinal ion transport, innate antimicrobial activity, cell-cell connection and transcription regulation.

Figures and Tables

Gene	Primer	Primer sequence	T_m	Main functions
Mouse GAPDH	*F49*	GGTGAAGGTCGGTGTGAACG/	48, 52 and 55°C	Reference gene
	R281	CTCGCTCCTGGAAGATGGTG		
Potassium intermediate/small conductance calcium-activated channel, subfamily N, member 4	*Kcnn4 F*	TCTGCACGCTAGATGTTGT/	55°C	Potassium ion transport
	Kcnn4 R	GACAAAGGAGGAAGGCAGTG		
Solute carrier family 12, member 2	*Nkcc1F*	CGATGAGCTGGAAAAGGAAC/	55°C	Sodium:potassium: chloride cotransport
	Nkcc1R	TGTATGCGACCACAGCATCT		
Solute carrier family 15 (H+/peptide transporter), member 2	*Slc15a2 F*	GGATGACAGCCATCAGGTTT/	55°C	Oligopeptide and proton transport
	Slc15a2R	TCCTCTTTGCACAGTTCTGTACTC		
Adenosine A2b receptor	*Adora2b F*	TGCTCACACAGAGCTCCATC/	55°C	G-protein coupled receptor protein signaling pathway
	Adora2b R	GTGTCCCAGTGACCAAACCT		
Solute carrier family 26, member 3	*Slc26a3 F*	GGCAAAATGATCGAAGCCATAGG/	55°C	Anion exchanger activity, transport
	Slc26a3R	GATGGTCCAGGAATGTCTTGTGATG		
Cldn 1 (Claudin1)	*Cldn1 F*	ACTGTGGATGTCCTGCGTTT/	55°C	Tight junctional protein
	Cldn1 R	CCAGCAGGATGCCAATTAC		
Cldn 5 (Claudin5)	*Cldn5 F*	CTGGACCACAACATCGTGAC/	55°C	Tight junctional protein
	Cldn5R	CAGATTCATACACCTTGCACTG		
Cldn7 (Claudin7)	*Cldn7 F*	CATGTACAAGGGGCTCTGGA/	55°C	Tight junctional protein
	Cldn7 R	GCTAAGAAGCCCAACACCAG		
Cldn 8 (Claudin8)	*Cldn8 F*	TGTCTGCCTTCATCGAAAGT/	55°C	Tight junctional protein
	Cldn8 R	GACCTTGCACTGCATTCTGA		
Aquaporin 1	*Aqp1 F*	AGCGAAATCAAGAAGAAGCTC/	48°C	Water transport
	Aqp1 R	CCTCTATTTGGCTTCATCTC		
Lectin, galactose binding, soluble 6	*Lgals6 F*	GTCCAACCTGTTGAAACCAA/	48°C	Carbohydrate recognition
	Lgals6 R	CCTATGTCCAGATCTGAGC		
Peroxisome proliferator-activated receptor gamma	*Ppar-γ F*	TTGCTGAACGTGAAGCCCATCGAGG	48°C	Regulation of fatty acid storage and glucose metabolism
	Ppar-γ R	GTCCTTGTAGATCTCCTGGAGCAG		
Nucleolin NH2	*Ncl F*	ATGGTGAARCTCGCAAAGGCHG/	48°C	Synthesis and maturation of ribosomes
	NclR	CAAAACCCACGGAGAGTC		
Intelectin	*Itln-1 F*	ATG ACC CAA CTG GGA TTC CTG/	52°C	Carbohydrate recognition
	Itln-1 R	TCA GCG ATA AAA CAG AAG CAC G		
mCRAMP	*Cnlp R*	CTTCAACCAGCAGTCCCTAGACA/	52°C	Cathelicidin-related antimicrobial peptide
	Cmlp R	TCCAGGTCCAGGAGACGGTA		
Galectin-4	*Gale4F3*	CAACCCTCCACAGATGAACACCTT/	52°C	Carbohydrate recognition
	Gale4R2	TCCAGCGTGTCTACCATTTGGAAT		
FBJ osteosarcoma oncogene B	*Fosb F*	TTCCTAGTGACACCTGAGAGCTG/	52°C	Regulation of transcription
	Fosb R	GAACATTGACGCTGAAGGACTAC		

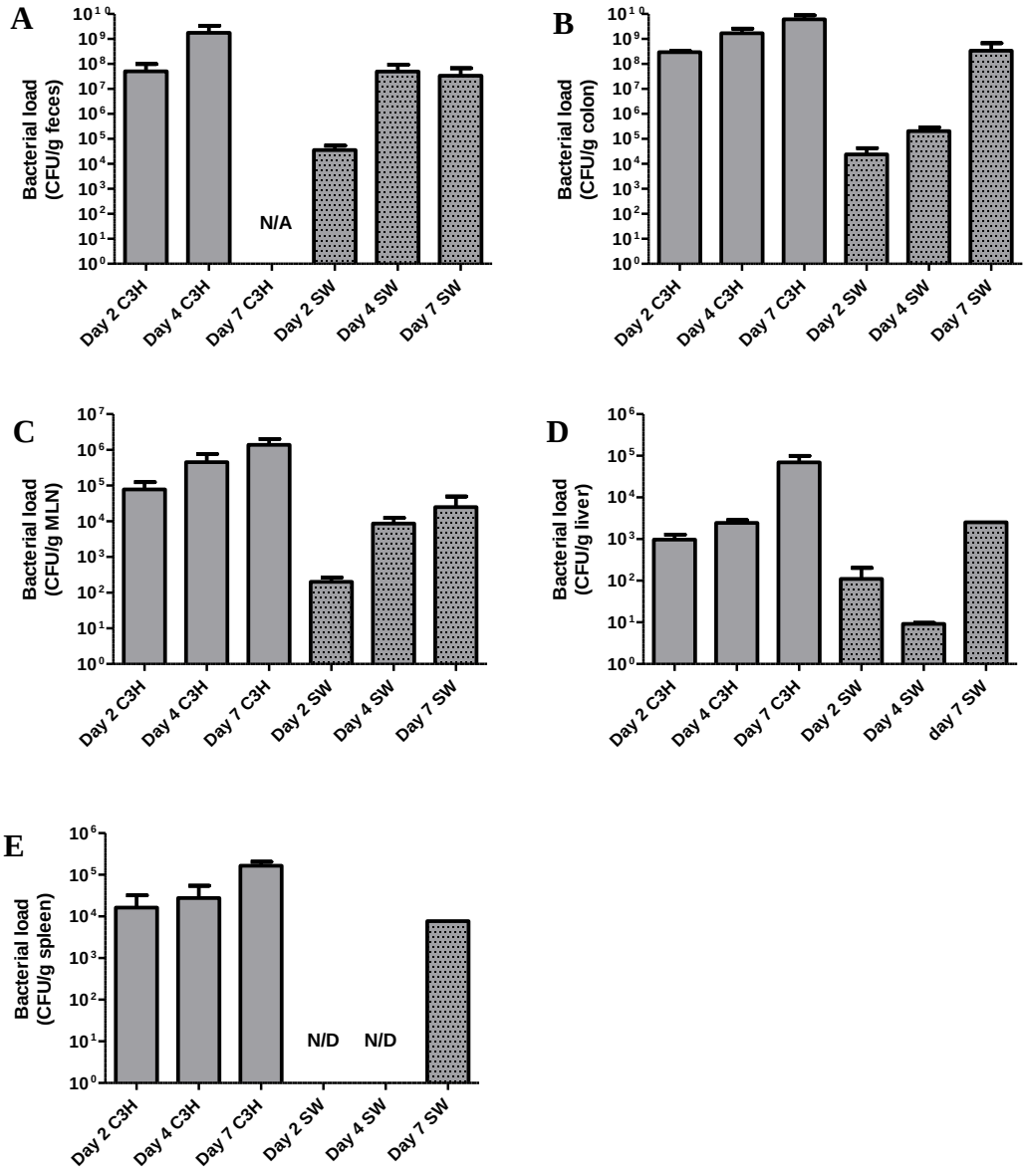

Figure 3-1 Bacterial enumeration in feces, colon MLN, liver and spleen of C3H and SW mice. Adjusted for day, bacterial loads in feces were higher in C3H mice than in SW mice (P <0.05) (A). Bacterial numbers colon, MLNs and liver of C3H mice were higher compared to SW mice (P < 0.0001) (B-D). When adjusted for mouse strain, bacterial numbers in feces and MLNs were higher at 4 and 7 dpi than at 2 dpi (P <0.001); bacterial loads in liver were higher at 7 dpi than on 2 and 4 dpi (P <0.001). Bacteria were undetectable in spleen of SW mice at 2 and 4 dpi and were not significantly different between C3H and SW mice at 7 dpi (E). N/A – not applicable, N/D – not determined.

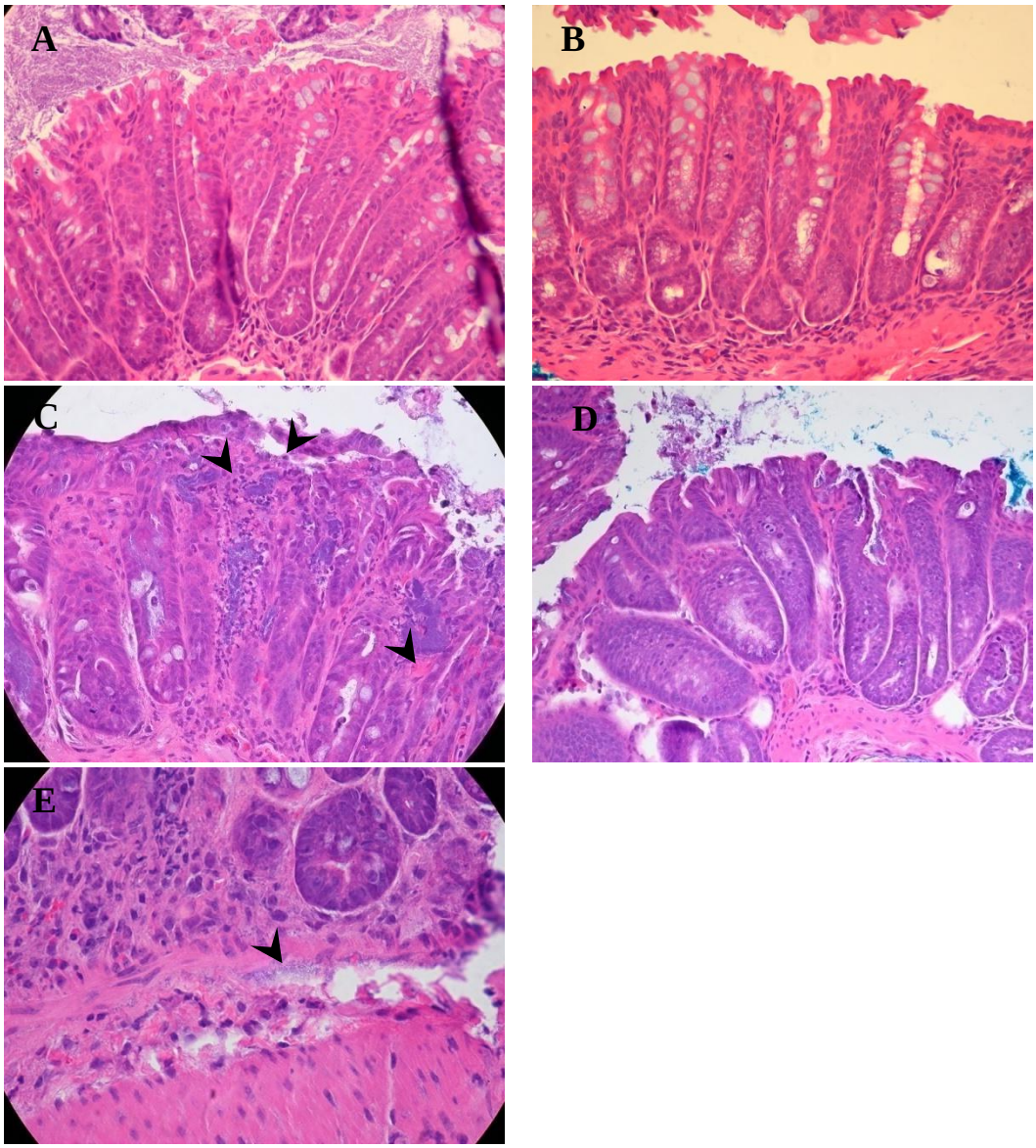

Figure 3-2 *C. rodentium* infection is heavier and leads to more severe colonic hyperplasia in susceptible mice.

At 2 dpi higher bacterial loads were observed in C3H mice (A) compared to SW mice (B). Strong mucosal inflammatory response, transmural colitis and blood congestion in C3H mice at 7 dpi (C). Ulceration and migration of bacteria into muscularis mucosa at 7 dpi in C3H mice (E). Mild to moderate inflammatory response with well preserved tissue morphology in SW mice at 7 dpi (D). Arrowheads indicate high bacterial loads (A), inflammatory cell infiltration ulceration, and hemorrhage (left to right, C) and bacteria in subepithelial colonic tissues (E). Magnifications: A-D, ×400; E, ×600.

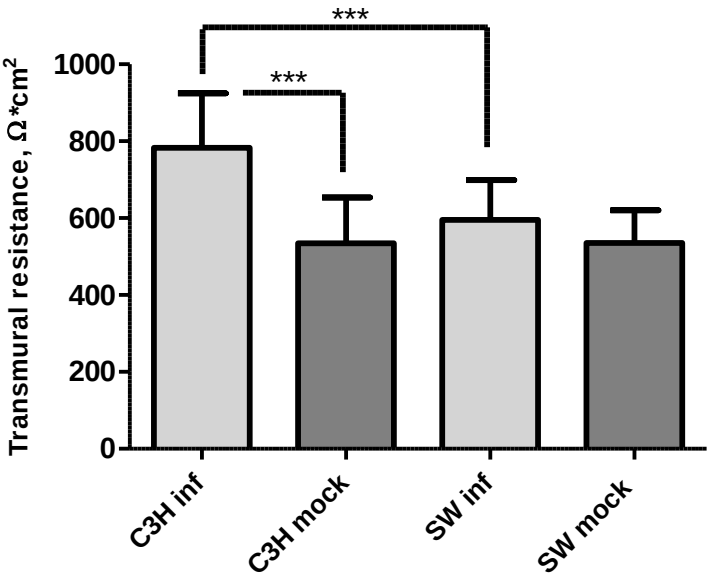

Figure 3-3 *C. rodentium* infection results in an increase of colonic R_{TE} of C3H mice.
The colonic R_{TE} of *C. rodentium*-inoculated C3H mice significantly increased compared to vehicle-inoculated C3H and *C. rodentium*-inoculated SW mice.
Each bar represents combined average from day 2 to 7. ***, P <0.0001

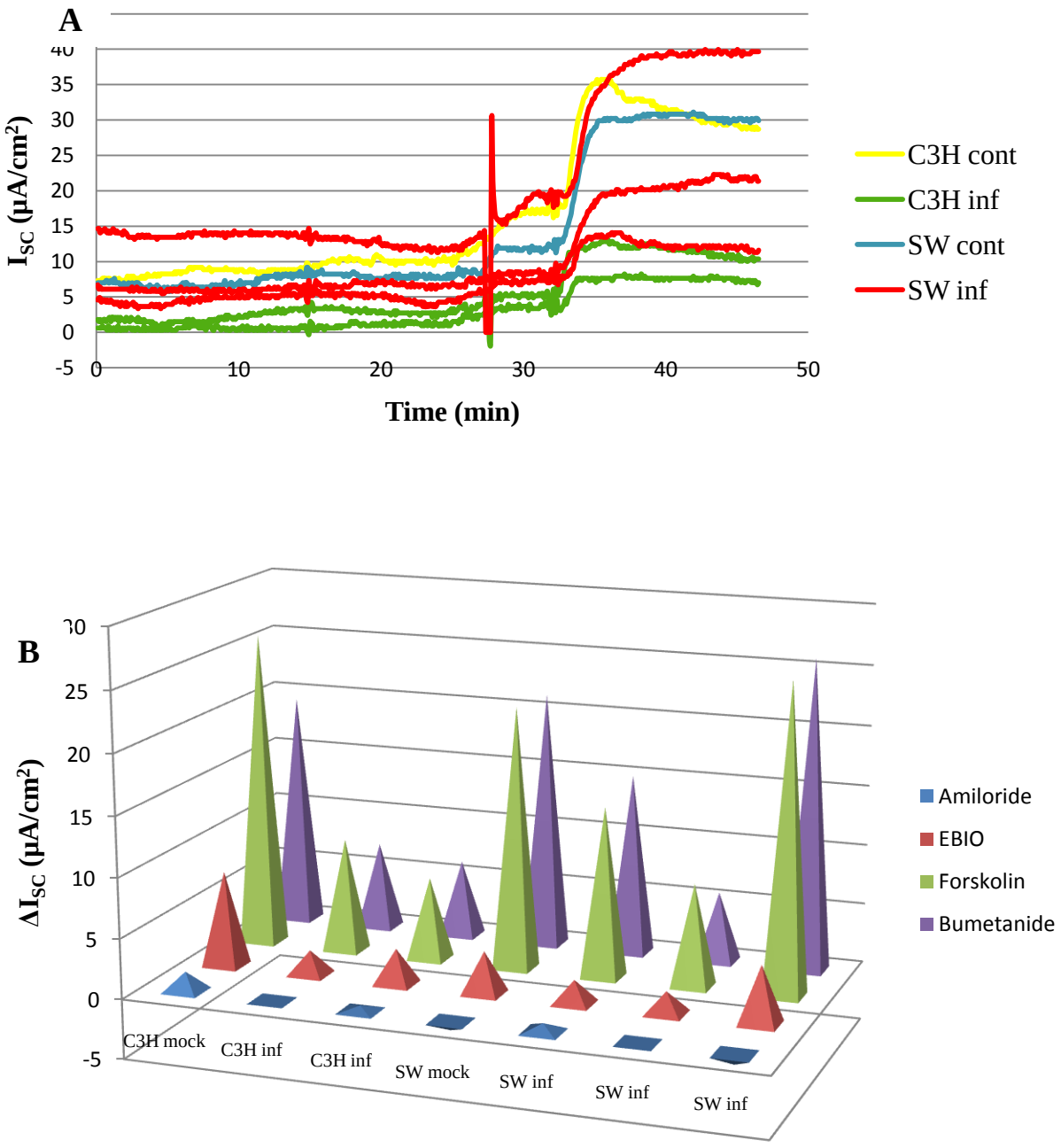

Figure 3-4. Effects of *C. rodentium* on transmural colonic short-circuit current (I_{SC}). Decreased basal short-circuit current responses at 4 dpi in the colon of *C. rodentium*-inoculated compared to vehicle-inoculated C3H mice (A). Changes of I_{SC} following treatment with amiloride, EBIO, forskolin and bumetanide, relative to basal I_{SC} (B).

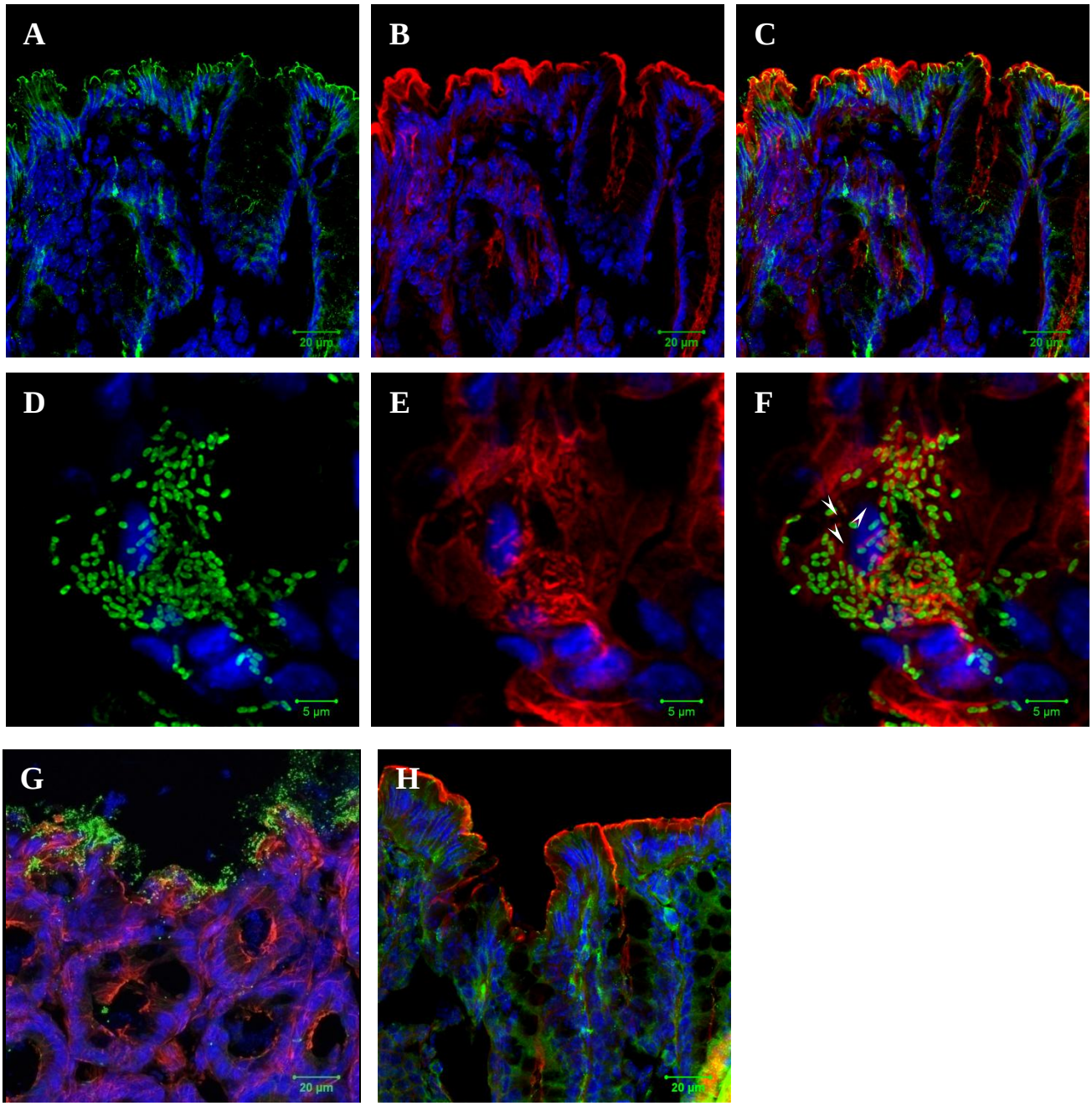
A
20 µm
B
20 µm
C
20 µm
D
5 µm
E
5 µm
F
5 µm
G
20 µm
H
20 µm

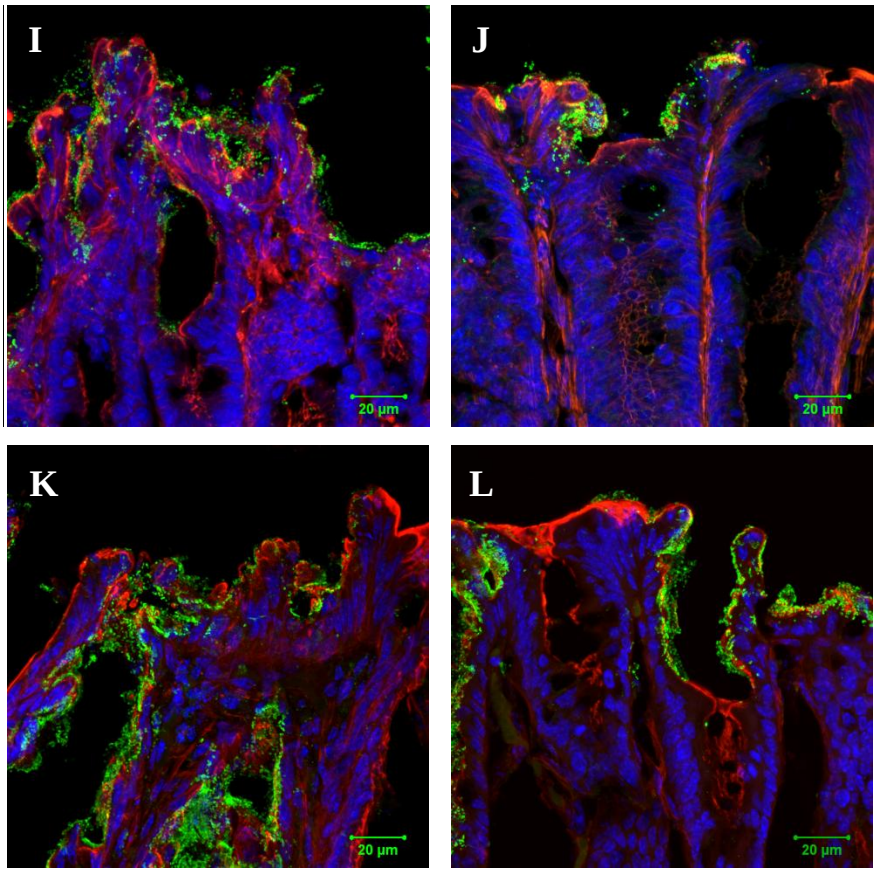

Figure 3-5 Redistribution of actin and occludin in the colon of mice inoculated with *C. rodentium.*

Normal distribution of actin (B) and occludin (A) in the mouse colon. Merged of A and B (C). Rearragement of actin (E) and occludin (D) into pedestals on the apical cell surface is well observed under higher magnification. Merged of D and E (F). Relocalization of occludin from TJ regions discretely at the apcal surface of colonic epithelial cells at 2 dpi in C3H (G); more normal occludin distribution in SW mice (H). Occludin reloclization in C3H and SW mice at 4 dpi (I and J respectively). Increase in pedestal formation in C3H (K) and SW (L) mice at 7 dpi. Actin is seen in red, occludin is seen in green, host cell nuclei are blue.

Arrowheads indicate colocalization of actin and occludin in pedestals.

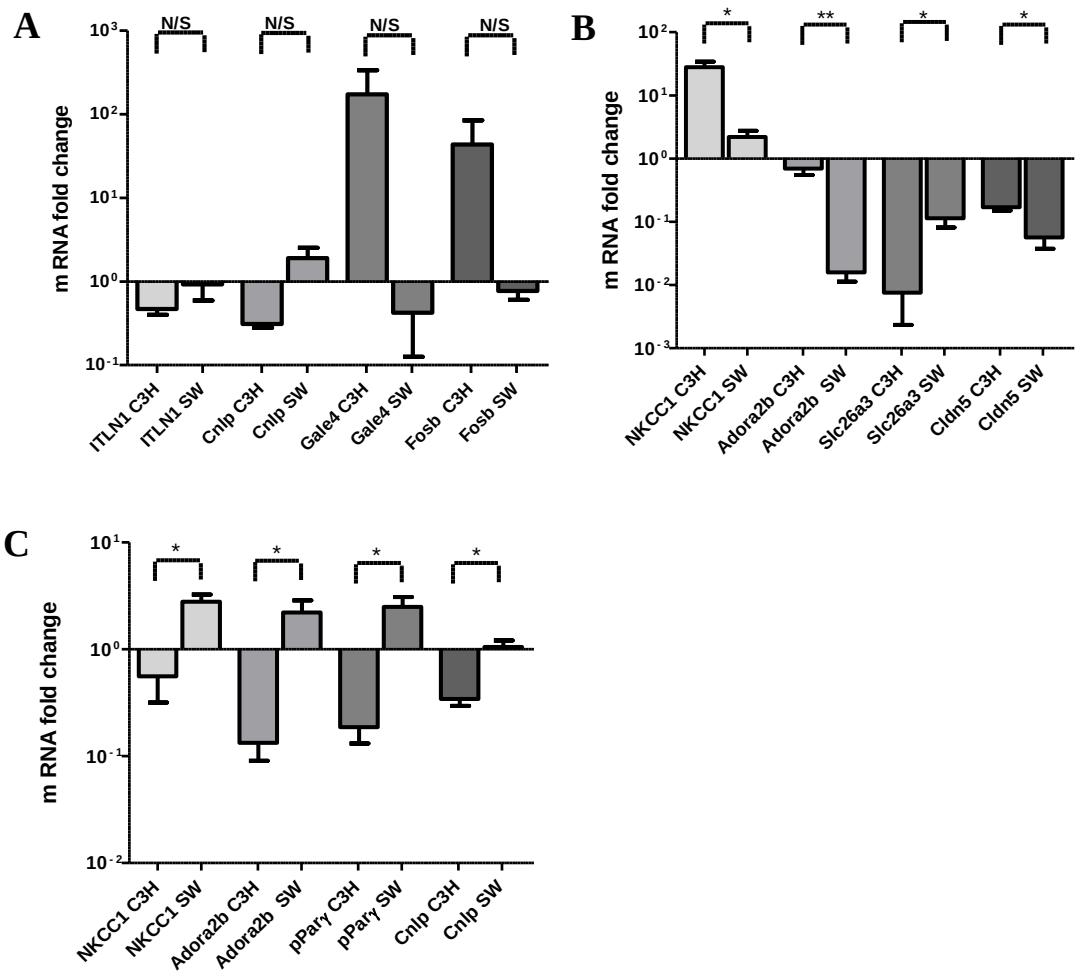

Figure 3-6 *C. rodentium* affects gene expression in murine colon.

Multiple genes were differentially expressed between infected C3H and SW mice at 2, 4 and 7 dpi (A, B and C respectively). The expression of genes was normalized to that of mock-infected C3H or SW mice. *, $P < 0.05$. **, $P < 0.01$. N/S – not significant.

Chapter 4 - Conclusion

Diarrheal diseases are a major problem worldwide but studying them can be complicated due to the lack of an appropriate *in vitro* or *in vivo* model. *C. rodentium* has been shown to induce pathological changes in epithelial cell cultures and diarrhea in mice, making this bacterium an ideal model for EPEC infections (97). Current research has been focused to identify bacterial virulence factors and host systems that contribute to the degree of severity of infection (23, 24, 36, 47, 134, 146). Innate and adaptive immunity, colonic secretion and absorption, and intestinal microbiota play an important role in the outcome of *C. rodentium* infection.

Recently published work revealed that transfer of microflora of resistant C57BL/6 to susceptible C3H/HeOuJ mice prior to infection fully protects the latter from fatal outcome. (55). Additionally, the Cri1, a locus controlling mortality during *C. rodentium* infection in mice was characterized. The transfer of this locus from resistant C57BL/6 to susceptible C3H/HeOuJ mice has been shown to decrease mortality (40). These studies indicate relevance of *C. rodentium* as a model organism for colonic inflammatory diseases, and support the relevance of research directed towards revealing mechanisms of EPEC-induced diarrhea.

The goals of the current work were to evaluate a *Ptk6* cell line as a new *in vitro* model for EPEC and EHEC infection, and to compare the changes that occur in the colon of susceptible and resistant mouse strains following intracecal inoculation with *C. rodentium*.

A unique *Ptk6* conditionally immortalized cell line was used to evaluate *C. rodentium*-induced changes in the colonic epithelium *in vitro*. *Ptk6* is a unique murine colonic cell line, which forms a polarized monolayer and exhibits a high R_{TE} when grown on Transwells (141). This study determined that *C. rodentium* attached to the *Ptk6* monolayers and induced the effacement of microvilli. Bacterial exposure induced loss of barrier properties of the monolayer,

characterized by decrease of R_{TE} and increased flux of macromolecules. Gene expression assays indicated potential dysregulation of ion transport, and an increased transcription of genes encoding for innate immunity factors. This study revealed that *C. rodentium*- associated changes in *Ptk6* cell culture resemble those occurring *in vivo* leading to the conclusion that the *Ptk6* cell line can be an ideal *in vitro* model for *C. rodentium* infection. *Ptk6* cell line has a unique capability to differentiate in to absorptive, goblet and neuriendocrine cells forming organoids when grown under specific conditions (141). Thus, future research can utilize this cell line to study the effect of *C. rodentium* on various cells that are present in the colonic epithelium.

In vivo studies attempted to compare *C. rodentium*-induced changes in the colonic epithelium of susceptible and resistant strains of mice. Bacteria were inoculated directly into the cecum, the part of the intestine in which C. *rodentium* colonizes first. As it has been reported previously (22, 130), C3H mice developed more severe clinical signs and tissue pathology than SW mice. We observed more significant disruption of epithelial morphology and function in C3H mice. These changes included the disturbance of cell cytoskeleton and occludin and changes in the expression of genes whose products are involved in the ion transport and in innate immune responses. Perhaps the most striking observation was the increase of colonic R_{TE} of *C. rodentium*-inoculated C3H mice, which may be associated with an increased area of tight epithelium. However, more studies need to be completed to identify underlying mechanisms to account for the R_{TE} increase. This study extends current knowledge regarding *C. rodentium* pathogenesis and suggests that a cumulative effect of multiple mechanisms may result in severe diarrhea and lead to death of susceptible mice.

In summary, it has been more than a decade since *C. rodentium* was recognized as a model pathogen for human colonic inflammatory diseases such as inflammatory bowel disease

(IBD) and EPEC infection. Importantly, *C. rodentium*-induced diarrhea is multi-factorial and therefore it is necessary to understand the relationship between different changes that occur in the intestine after the infection such as the relationship between inflammation, secretion, absorption and TJs. The establishment of a new cell culture model could be a good starting point to for studying *C. rodentium* pathogenesis, while *in vivo* studies on various mouse models should be used to determine multiple bacterial and host factors involved in disease progression to provide insight on intestinal physiology and approaches for management of diarrhea.

Chapter 5 - References

1. , posting date. Diarrheagenic Escherichia coli. Technical information. http://www.cdc.gov/nczved/divisions/dfbmd/diseases/diarrheagenic_ecoli/technical.html#incidence. [Online.]
2. **Al-Sadi, R., M. Boivin, and T. Ma.** 2009. Mechanism of cytokine modulation of epithelial tight junction barrier. Front Biosci **14:**2765-2778.
3. **Al-Sadi, R., K. Khatib, S. Guo, D. Ye, M. Youssef, and T. Y. Ma.** Occludin Regulates Macromolecule Flux across the Intestinal Epithelial Tight Junction Barrier. Am J Physiol Gastrointest Liver Physiol.
4. **Amasheh, S., T. Schmidt, M. Mahn, P. Florian, J. Mankertz, S. Tavalali, A. H. Gitter, J. D. Schulzke, and M. Fromm.** 2005. Contribution of claudin-5 to barrier properties in tight junctions of epithelial cells. Cell Tissue Res **321:**89-96.
5. **Anderson, J. M., and C. M. Van Itallie.** 2009. Physiology and function of the tight junction. Cold Spring Harb Perspect Biol **1:**a002584.
6. **Antunes, L. C., R. B. Ferreira, M. M. Buckner, and B. B. Finlay.** Quorum sensing in bacterial virulence. Microbiology **156:**2271-2282.
7. **Arnold, R., A. Jehl, and T. Rattei.** Targeting effectors: the molecular recognition of Type III secreted proteins. Microbes Infect **12:**346-358.
8. **Asad, S., and S. M. Opal.** 2008. Bench-to-bedside review: Quorum sensing and the role of cell-to-cell communication during invasive bacterial infection. Crit Care **12:**236.
9. **Babbin, B. A., M. Sasaki, K. W. Gerner-Schmidt, A. Nusrat, and J. M. Klapproth.** 2009. The bacterial virulence factor lymphostatin compromises intestinal epithelial barrier function by modulating rho GTPases. Am J Pathol **174:**1347-1357.
10. **Balda, M. S., J. A. Whitney, C. Flores, S. Gonzalez, M. Cereijido, and K. Matter.** 1996. Functional dissociation of paracellular permeability and transepithelial electrical resistance and disruption of the apical-basolateral intramembrane diffusion barrier by expression of a mutant tight junction membrane protein. J Cell Biol **134:**1031-1049.
11. **Barrett, K. E., and S. J. Keely.** 2000. Chloride secretion by the intestinal epithelium: molecular basis and regulatory aspects. Annu Rev Physiol **62:**535-572.
12. **Barthold, S. W., G. L. Coleman, R. O. Jacoby, E. M. Livestone, and A. M. Jonas.** 1978. Transmissible murine colonic hyperplasia. Vet Pathol **15:**223-236.
13. **Bauer, H. C., A. Traweger, J. Zweimueller-Mayer, C. Lehner, H. Tempfer, I. Krizbai, I. Wilhelm, and H. Bauer.** New aspects of the molecular constituents of tissue barriers. J Neural Transm **118:**7-21.
14. **Bergstrom, K. S., J. A. Guttman, M. Rumi, C. Ma, S. Bouzari, M. A. Khan, D. L. Gibson, A. W. Vogl, and B. A. Vallance.** 2008. Modulation of intestinal goblet cell function during infection by an attaching and effacing bacterial pathogen. Infect Immun **76:**796-811.
15. **Bergstrom, K. S., V. Kissoon-Singh, D. L. Gibson, C. Ma, M. Montero, H. P. Sham, N. Ryz, T. Huang, A. Velcich, B. B. Finlay, K. Chadee, and B. A. Vallance.** Muc2 protects against lethal infectious colitis by disassociating pathogenic and commensal bacteria from the colonic mucosa. PLoS Pathog **6:**e1000902.

16. **Berkes, J., V. K. Viswanathan, S. D. Savkovic, and G. Hecht.** 2003. Intestinal epithelial responses to enteric pathogens: effects on the tight junction barrier, ion transport, and inflammation. Gut **52:**439-451.
17. **Binder, H. J.** 2009. Mechanisms of diarrhea in inflammatory bowel diseases. Ann N Y Acad Sci **1165:**285-293.
18. **Bishop, A. L., S. Wiles, G. Dougan, and G. Frankel.** 2007. Cell attachment properties and infectivity of host-adapted and environmentally adapted Citrobacter rodentium. Microbes Infect **9:**1316-1324.
19. **Bleichner, G., H. Blehaut, H. Mentec, and D. Moyse.** 1997. Saccharomyces boulardii prevents diarrhea in critically ill tube-fed patients. A multicenter, randomized, double-blind placebo-controlled trial. Intensive Care Med **23:**517-523.
20. **Borenshtein, D., R. C. Fry, E. B. Groff, P. R. Nambiar, V. J. Carey, J. G. Fox, and D. B. Schauer.** 2008. Diarrhea as a cause of mortality in a mouse model of infectious colitis. Genome Biol **9:**R122.
21. **Borenshtein, D., P. R. Nambiar, E. B. Groff, J. G. Fox, and D. B. Schauer.** 2007. Development of fatal colitis in FVB mice infected with Citrobacter rodentium. Infect Immun **75:**3271-3281.
22. **Borenshtein, D., K. A. Schlieper, B. H. Rickman, J. M. Chapman, C. W. Schweinfest, J. G. Fox, and D. B. Schauer.** 2009. Decreased expression of colonic Slc26a3 and carbonic anhydrase iv as a cause of fatal infectious diarrhea in mice. Infect Immun **77:**3639-3650.
23. **Brereton, C. F., and J. M. Blander.** Responding to infection and apoptosis--a task for TH17 cells. Ann N Y Acad Sci **1209:**56-67.
24. **Brown, J. B., P. Cheresh, T. Goretsky, E. Managlia, G. R. Grimm, H. Ryu, M. Zadeh, R. Dirisina, and T. A. Barrett.** Epithelial PI3K signaling is required for {beta}-catenin activation and host defense against Citrobacter rodentium infection. Infect Immun.
25. **Bry, L., and M. B. Brenner.** 2004. Critical role of T cell-dependent serum antibody, but not the gut-associated lymphoid tissue, for surviving acute mucosal infection with Citrobacter rodentium, an attaching and effacing pathogen. J Immunol **172:**433-441.
26. **Bry, L., M. Brigl, and M. B. Brenner.** 2006. CD4+-T-cell effector functions and costimulatory requirements essential for surviving mucosal infection with Citrobacter rodentium. Infect Immun **74:**673-681.
27. **Chen, C. C., C. H. Chiu, T. Y. Lin, H. N. Shi, and W. A. Walker.** 2009. Effect of probiotics Lactobacillus acidophilus on Citrobacter rodentium colitis: the role of dendritic cells. Pediatr Res **65:**169-175.
28. **Conlin, V. S., X. Wu, C. Nguyen, C. Dai, B. A. Vallance, A. M. Buchan, L. Boyer, and K. Jacobson.** 2009. Vasoactive intestinal peptide ameliorates intestinal barrier disruption associated with Citrobacter rodentium-induced colitis. Am J Physiol Gastrointest Liver Physiol **297:**G735-750.
29. **Cordone, A., E. M. Mauriello, D. J. Pickard, G. Dougan, M. De Felice, and E. Ricca.** 2005. The lrp gene and its role in type I fimbriation in Citrobacter rodentium. J Bacteriol **187:**7009-7017.
30. **Coulthurst, S. J., S. Clare, T. J. Evans, I. J. Foulds, K. J. Roberts, M. Welch, G. Dougan, and G. P. Salmond.** 2007. Quorum sensing has an unexpected role in virulence in the model pathogen Citrobacter rodentium. EMBO Rep **8:**698-703.

31. **Crepin, V. F., F. Girard, S. Schuller, A. D. Phillips, A. Mousnier, and G. Frankel.** Dissecting the role of the Tir:Nck and Tir:IRTKS/IRSp53 signalling pathways in vivo. Mol Microbiol **75:**308-323.
32. **Croxen, M. A., and B. B. Finlay.** Molecular mechanisms of Escherichia coli pathogenicity. Nat Rev Microbiol **8:**26-38.
33. **D'Arienzo, R., F. Maurano, G. Mazzarella, D. Luongo, R. Stefanile, E. Ricca, and M. Rossi.** 2006. Bacillus subtilis spores reduce susceptibility to Citrobacter rodentium-mediated enteropathy in a mouse model. Res Microbiol **157:**891-897.
34. **Dean, P., and B. Kenny.** 2004. Intestinal barrier dysfunction by enteropathogenic Escherichia coli is mediated by two effector molecules and a bacterial surface protein. Mol Microbiol **54:**665-675.
35. **Deng, W., Y. Li, B. A. Vallance, and B. B. Finlay.** 2001. Locus of enterocyte effacement from Citrobacter rodentium: sequence analysis and evidence for horizontal transfer among attaching and effacing pathogens. Infect Immun **69:**6323-6335.
36. **Deng, W., J. L. Puente, S. Gruenheid, Y. Li, B. A. Vallance, A. Vazquez, J. Barba, J. A. Ibarra, P. O'Donnell, P. Metalnikov, K. Ashman, S. Lee, D. Goode, T. Pawson, and B. B. Finlay.** 2004. Dissecting virulence: systematic and functional analyses of a pathogenicity island. Proc Natl Acad Sci U S A **101:**3597-3602.
37. **Deng, W., B. A. Vallance, Y. Li, J. L. Puente, and B. B. Finlay.** 2003. Citrobacter rodentium translocated intimin receptor (Tir) is an essential virulence factor needed for actin condensation, intestinal colonization and colonic hyperplasia in mice. Mol Microbiol **48:**95-115.
38. **Derikx, J. P., M. D. Luyer, E. Heineman, and W. A. Buurman.** Non-invasive markers of gut wall integrity in health and disease. World J Gastroenterol **16:**5272-5279.
39. **Di Cagno, R., M. De Angelis, M. Calasso, and M. Gobbetti.** Proteomics of the bacterial cross-talk by quorum sensing. J Proteomics **74:**19-34.
40. **Diez, E., L. Zhu, S. A. Teatero, M. Paquet, M. F. Roy, J. C. Loredo-Osti, D. Malo, and S. Gruenheid.** Identification and characterization of Cri1, a locus controlling mortality during Citrobacter rodentium infection in mice. Genes Immun.
41. **Dong, T., B. K. Coombes, and H. E. Schellhorn.** 2009. Role of RpoS in the virulence of Citrobacter rodentium. Infect Immun **77:**501-507.
42. **Ebnet, K.** 2008. Organization of multiprotein complexes at cell-cell junctions. Histochem Cell Biol **130:**1-20.
43. **Findley, M. K., and M. Koval.** 2009. Regulation and roles for claudin-family tight junction proteins. IUBMB Life **61:**431-437.
44. **Flynn, A. N., and A. G. Buret.** 2008. Tight junctional disruption and apoptosis in an in vitro model of Citrobacter rodentium infection. Microb Pathog **45:**98-104.
45. **Forster, C.** 2008. Tight junctions and the modulation of barrier function in disease. Histochem Cell Biol **130:**55-70.
46. **Frankel, G., O. Lider, R. Hershkoviz, A. P. Mould, S. G. Kachalsky, D. C. Candy, L. Cahalon, M. J. Humphries, and G. Dougan.** 1996. The cell-binding domain of intimin from enteropathogenic Escherichia coli binds to beta1 integrins. J Biol Chem **271:**20359-20364.
47. **Frankel, G., A. D. Phillips, M. Novakova, H. Field, D. C. Candy, D. B. Schauer, G. Douce, and G. Dougan.** 1996. Intimin from enteropathogenic Escherichia coli restores

murine virulence to a Citrobacter rodentium eaeA mutant: induction of an immunoglobulin A response to intimin and EspB. Infect Immun **64:**5315-5325.

48. **Frankel, G., A. D. Phillips, L. R. Trabulsi, S. Knutton, G. Dougan, and S. Matthews.** 2001. Intimin and the host cell--is it bound to end in Tir(s)? Trends Microbiol **9:**214-218.
49. **Gallo, R. L., K. J. Kim, M. Bernfield, C. A. Kozak, M. Zanetti, L. Merluzzi, and R. Gennaro.** 1997. Identification of CRAMP, a cathelin-related antimicrobial peptide expressed in the embryonic and adult mouse. J Biol Chem **272:**13088-13093.
50. **Galloway, W. R., J. T. Hodgkinson, S. D. Bowden, M. Welch, and D. R. Spring.** Quorum sensing in Gram-negative bacteria: small-molecule modulation of AHL and AI-2 quorum sensing pathways. Chem Rev **111:**28-67.
51. **Garduno, J., E. Galvan, D. Fernandez de Sevilla, and W. Buno.** 2005. 1-Ethyl-2-benzimidazolinone (EBIO) suppresses epileptiform activity in in vitro hippocampus. Neuropharmacology **49:**376-388.
52. **Gareau, M. G., E. Wine, C. Reardon, and P. M. Sherman.** Probiotics prevent death caused by Citrobacter rodentium infection in neonatal mice. J Infect Dis **201:**81-91.
53. **Garmendia, J., G. Frankel, and V. F. Crepin.** 2005. Enteropathogenic and enterohemorrhagic Escherichia coli infections: translocation, translocation, translocation. Infect Immun **73:**2573-2585.
54. **Geibel, J. P.** 2005. Secretion and absorption by colonic crypts. Annu Rev Physiol **67:**471-490.
55. **Ghosh, S., C. Dai, K. Brown, E. Rajendiran, S. Makarenko, J. Baker, C. Ma, S. Halder, M. Montero, V. A. Ionescu, A. Klegeris, B. A. Vallance, and D. L. Gibson.** Colonic microbiota alters host susceptibility to infectious colitis by modulating inflammation, redox status and ion transporter gene expression. Am J Physiol Gastrointest Liver Physiol.
56. **Gibson, D. L., C. Ma, K. S. Bergstrom, J. T. Huang, C. Man, and B. A. Vallance.** 2008. MyD88 signalling plays a critical role in host defence by controlling pathogen burden and promoting epithelial cell homeostasis during Citrobacter rodentium-induced colitis. Cell Microbiol **10:**618-631.
57. **Gill, R. K., A. Borthakur, K. Hodges, J. R. Turner, D. R. Clayburgh, S. Saksena, A. Zaheer, K. Ramaswamy, G. Hecht, and P. K. Dudeja.** 2007. Mechanism underlying inhibition of intestinal apical Cl/OH exchange following infection with enteropathogenic E. coli. J Clin Invest **117:**428-437.
58. **Gitter, A. H., K. Bendfeldt, J. D. Schulzke, and M. Fromm.** 2000. Trans/paracellular, surface/crypt, and epithelial/subepithelial resistances of mammalian colonic epithelia. Pflugers Arch **439:**477-482.
59. **Gonzalez-Mariscal, L., A. Betanzos, P. Nava, and B. E. Jaramillo.** 2003. Tight junction proteins. Prog Biophys Mol Biol **81:**1-44.
60. **Guslandi, M., P. Giollo, and P. A. Testoni.** 2003. A pilot trial of Saccharomyces boulardii in ulcerative colitis. Eur J Gastroenterol Hepatol **15:**697-698.
61. **Guslandi, M., G. Mezzi, M. Sorghi, and P. A. Testoni.** 2000. Saccharomyces boulardii in maintenance treatment of Crohn's disease. Dig Dis Sci **45:**1462-1464.
62. **Guttman, J. A., Y. Li, M. E. Wickham, W. Deng, A. W. Vogl, and B. B. Finlay.** 2006. Attaching and effacing pathogen-induced tight junction disruption in vivo. Cell Microbiol **8:**634-645.

63. **Guttman, J. A., F. N. Samji, Y. Li, A. W. Vogl, and B. B. Finlay.** 2006. Evidence that tight junctions are disrupted due to intimate bacterial contact and not inflammation during attaching and effacing pathogen infection in vivo. Infect Immun **74:**6075-6084.
64. **Hansson, G. C., and M. E. Johansson.** The inner of the two Muc2 mucin-dependent mucus layers in colon is devoid of bacteria. Gut Microbes **1:**51-54.
65. **Hase, K., L. Eckmann, J. D. Leopard, N. Varki, and M. F. Kagnoff.** 2002. Cell differentiation is a key determinant of cathelicidin LL-37/human cationic antimicrobial protein 18 expression by human colon epithelium. Infect Immun **70:**953-963.
66. **Hase, K., M. Murakami, M. Iimura, S. P. Cole, Y. Horibe, T. Ohtake, M. Obonyo, R. L. Gallo, L. Eckmann, and M. F. Kagnoff.** 2003. Expression of LL-37 by human gastric epithelial cells as a potential host defense mechanism against Helicobacter pylori. Gastroenterology **125:**1613-1625.
67. **Hecht, G., K. Hodges, R. K. Gill, F. Kear, S. Tyagi, J. Malakooti, K. Ramaswamy, and P. K. Dudeja.** 2004. Differential regulation of Na+/H+ exchange isoform activities by enteropathogenic E. coli in human intestinal epithelial cells. Am J Physiol Gastrointest Liver Physiol **287:**G370-378.
68. **Hecht, G., and A. Koutsouris.** 1999. Enteropathogenic E. coli attenuates secretagogue-induced net intestinal ion transport but not Cl- secretion. Am J Physiol **276:**G781-788.
69. **Hengge, R.** 2009. Proteolysis of sigmaS (RpoS) and the general stress response in Escherichia coli. Res Microbiol **160:**667-676.
70. **Higgins, L. M., G. Frankel, I. Connerton, N. S. Goncalves, G. Dougan, and T. T. MacDonald.** 1999. Role of bacterial intimin in colonic hyperplasia and inflammation. Science **285:**588-591.
71. **Higgins, L. M., G. Frankel, G. Douce, G. Dougan, and T. T. MacDonald.** 1999. Citrobacter rodentium infection in mice elicits a mucosal Th1 cytokine response and lesions similar to those in murine inflammatory bowel disease. Infect Immun **67:**3031-3039.
72. **Hodges, K., N. M. Alto, K. Ramaswamy, P. K. Dudeja, and G. Hecht.** 2008. The enteropathogenic Escherichia coli effector protein EspF decreases sodium hydrogen exchanger 3 activity. Cell Microbiol **10:**1735-1745.
73. **Hodges, K., and R. Gill.** Infectious diarrhea: Cellular and molecular mechanisms. Gut Microbes **1:**4-21.
74. **Hou, J., A. Renigunta, M. Konrad, A. S. Gomes, E. E. Schneeberger, D. L. Paul, S. Waldegger, and D. A. Goodenough.** 2008. Claudin-16 and claudin-19 interact and form a cation-selective tight junction complex. J Clin Invest **118:**619-628.
75. **Iimura, M., R. L. Gallo, K. Hase, Y. Miyamoto, L. Eckmann, and M. F. Kagnoff.** 2005. Cathelicidin mediates innate intestinal defense against colonization with epithelial adherent bacterial pathogens. J Immunol **174:**4901-4907.
76. **Ishigame, H., S. Kakuta, T. Nagai, M. Kadoki, A. Nambu, Y. Komiyama, N. Fujikado, Y. Tanahashi, A. Akitsu, H. Kotaki, K. Sudo, S. Nakae, C. Sasakawa, and Y. Iwakura.** 2009. Differential roles of interleukin-17A and -17F in host defense against mucoepithelial bacterial infection and allergic responses. Immunity **30:**108-119.
77. **Itoh, T., H. Doi, S. Chin, T. Nishimura, and S. Kasahara.** 1988. Establishment of mouse thymic nurse cell clones from a spontaneous BALB/c thymic tumor. Eur J Immunol **18:**821-824.

78. **Jennings, M. E., L. N. Quick, A. Soni, R. R. Davis, K. Crosby, C. M. Ott, C. A. Nickerson, and J. W. Wilson.** Characterization of the Salmonella enterica serovar Typhimurium ydcI gene which encodes a conserved DNA binding protein required for full acid stress resistance. J Bacteriol.
79. **Johnson-Henry, K. C., M. Nadjafi, Y. Avitzur, D. J. Mitchell, B. Y. Ngan, E. Galindo-Mata, N. L. Jones, and P. M. Sherman.** 2005. Amelioration of the effects of Citrobacter rodentium infection in mice by pretreatment with probiotics. J Infect Dis **191:**2106-2117.
80. **Johnson, E., and S. W. Barthold.** 1979. The ultrastructure of transmissible murine colonic hyperplasia. Am J Pathol **97:**291-313.
81. **Klapproth, J. M.** 2010. The Role of Lymphostatin/EHEC Factor for Adherence-1 in the Pathogenesis of Gram Negative Infection. Toxins **2:**954-962.
82. **Klapproth, J. M., and F. Meyer.** 2009. [Multitalented lymphostatin]. Dtsch Med Wochenschr **134:**417-420.
83. **Klapproth, J. M., M. Sasaki, M. Sherman, B. Babbin, M. S. Donnenberg, P. J. Fernandes, I. C. Scaletsky, D. Kalman, A. Nusrat, and I. R. Williams.** 2005. Citrobacter rodentium lifA/efa1 is essential for colonic colonization and crypt cell hyperplasia in vivo. Infect Immun **73:**1441-1451.
84. **Kunzelmann, K., and M. Mall.** 2002. Electrolyte transport in the mammalian colon: mechanisms and implications for disease. Physiol Rev **82:**245-289.
85. **Lee, A. S., D. L. Gibson, Y. Zhang, H. P. Sham, B. A. Vallance, and J. P. Dutz.** Gut barrier disruption by an enteric bacterial pathogen accelerates insulitis in NOD mice. Diabetologia **53:**741-748.
86. **Lee, P. H., T. Ohtake, M. Zaiou, M. Murakami, J. A. Rudisill, K. H. Lin, and R. L. Gallo.** 2005. Expression of an additional cathelicidin antimicrobial peptide protects against bacterial skin infection. Proc Natl Acad Sci U S A **102:**3750-3755.
87. **Li, Q., Q. Zhang, C. Wang, N. Li, and J. Li.** 2008. Invasion of enteropathogenic Escherichia coli into host cells through epithelial tight junctions. FEBS J **275:**6022-6032.
88. **Luperchio, S. A., J. V. Newman, C. A. Dangler, M. D. Schrenzel, D. J. Brenner, A. G. Steigerwalt, and D. B. Schauer.** 2000. Citrobacter rodentium, the causative agent of transmissible murine colonic hyperplasia, exhibits clonality: synonymy of C. rodentium and mouse-pathogenic Escherichia coli. J Clin Microbiol **38:**4343-4350.
89. **Luperchio, S. A., and D. B. Schauer.** 2001. Molecular pathogenesis of Citrobacter rodentium and transmissible murine colonic hyperplasia. Microbes Infect **3:**333-340.
90. **Ma, C., M. E. Wickham, J. A. Guttman, W. Deng, J. Walker, K. L. Madsen, K. Jacobson, W. A. Vogl, B. B. Finlay, and B. A. Vallance.** 2006. Citrobacter rodentium infection causes both mitochondrial dysfunction and intestinal epithelial barrier disruption in vivo: role of mitochondrial associated protein (Map). Cell Microbiol **8:**1669-1686.
91. **Maaser, C., M. P. Housley, M. Iimura, J. R. Smith, B. A. Vallance, B. B. Finlay, J. R. Schreiber, N. M. Varki, M. F. Kagnoff, and L. Eckmann.** 2004. Clearance of Citrobacter rodentium requires B cells but not secretory immunoglobulin A (IgA) or IgM antibodies. Infect Immun **72:**3315-3324.
92. **Mangan, P. R., L. E. Harrington, D. B. O'Quinn, W. S. Helms, D. C. Bullard, C. O. Elson, R. D. Hatton, S. M. Wahl, T. R. Schoeb, and C. T. Weaver.** 2006.

Transforming growth factor-beta induces development of the T(H)17 lineage. Nature **441:**231-234.

93. **Martin, J., P. Malreddy, T. Iwamoto, L. C. Freeman, H. J. Davidson, J. M. Tomich, and B. D. Schultz.** 2009. NC-1059: a channel-forming peptide that modulates drug delivery across in vitro corneal epithelium. Invest Ophthalmol Vis Sci **50:**3337-3345.
94. **Martinez-Augustin, O., I. Romero-Calvo, M. D. Suarez, A. Zarzuelo, and F. S. de Medina.** 2009. Molecular bases of impaired water and ion movements in inflammatory bowel diseases. Inflamm Bowel Dis **15:**114-127.
95. **Maruthamuthu, V., Y. Aratyn-Schaus, and M. L. Gardel.** Conserved F-actin dynamics and force transmission at cell adhesions. Curr Opin Cell Biol **22:**583-588.
96. **Mudgett, M. B.** 2005. New insights to the function of phytopathogenic bacterial type III effectors in plants. Annu Rev Plant Biol **56:**509-531.
97. **Mundy, R., F. Girard, A. J. FitzGerald, and G. Frankel.** 2006. Comparison of colonization dynamics and pathology of mice infected with enteropathogenic Escherichia coli, enterohaemorrhagic E. coli and Citrobacter rodentium. FEMS Microbiol Lett **265:**126-132.
98. **Mundy, R., T. T. MacDonald, G. Dougan, G. Frankel, and S. Wiles.** 2005. Citrobacter rodentium of mice and man. Cell Microbiol **7:**1697-1706.
99. **Mundy, R., L. Petrovska, K. Smollett, N. Simpson, R. K. Wilson, J. Yu, X. Tu, I. Rosenshine, S. Clare, G. Dougan, and G. Frankel.** 2004. Identification of a novel Citrobacter rodentium type III secreted protein, EspI, and roles of this and other secreted proteins in infection. Infect Immun **72:**2288-2302.
100. **Mundy, R., D. Pickard, R. K. Wilson, C. P. Simmons, G. Dougan, and G. Frankel.** 2003. Identification of a novel type IV pilus gene cluster required for gastrointestinal colonization of Citrobacter rodentium. Mol Microbiol **48:**795-809.
101. **Mundy, R., S. Schuller, F. Girard, J. M. Fairbrother, A. D. Phillips, and G. Frankel.** 2007. Functional studies of intimin in vivo and ex vivo: implications for host specificity and tissue tropism. Microbiology **153:**959-967.
102. **Muza-Moons, M. M., E. E. Schneeberger, and G. A. Hecht.** 2004. Enteropathogenic Escherichia coli infection leads to appearance of aberrant tight junctions strands in the lateral membrane of intestinal epithelial cells. Cell Microbiol **6:**783-793.
103. **Newman, J. V., B. A. Zabel, S. S. Jha, and D. B. Schauer.** 1999. Citrobacter rodentium espB is necessary for signal transduction and for infection of laboratory mice. Infect Immun **67:**6019-6025.
104. **Peralta-Ramirez, J., J. M. Hernandez, R. Manning-Cela, J. Luna-Munoz, C. Garcia-Tovar, J. P. Nougayrede, E. Oswald, and F. Navarro-Garcia.** 2008. EspF Interacts with nucleation-promoting factors to recruit junctional proteins into pedestals for pedestal maturation and disruption of paracellular permeability. Infect Immun **76:**3854-3868.
105. **Pestonjamasp, V. K., K. H. Huttner, and R. L. Gallo.** 2001. Processing site and gene structure for the murine antimicrobial peptide CRAMP. Peptides **22:**1643-1650.
106. **Petty, N. K., R. Bulgin, V. F. Crepin, A. M. Cerdeno-Tarraga, G. N. Schroeder, M. A. Quail, N. Lennard, C. Corton, A. Barron, L. Clark, A. L. Toribio, J. Parkhill, G. Dougan, G. Frankel, and N. R. Thomson.** The Citrobacter rodentium genome sequence reveals convergent evolution with human pathogenic Escherichia coli. J Bacteriol **192:**525-538.

107. **Philpott, D. J., D. M. McKay, P. M. Sherman, and M. H. Perdue.** 1996. Infection of T84 cells with enteropathogenic Escherichia coli alters barrier and transport functions. Am J Physiol **270:**G634-645.
108. **Ramanathan, B., E. G. Davis, C. R. Ross, and F. Blecha.** 2002. Cathelicidins: microbicidal activity, mechanisms of action, and roles in innate immunity. Microbes Infect **4:**361-372.
109. **Saitou, M., K. Fujimoto, Y. Doi, M. Itoh, T. Fujimoto, M. Furuse, H. Takano, T. Noda, and S. Tsukita.** 1998. Occludin-deficient embryonic stem cells can differentiate into polarized epithelial cells bearing tight junctions. J Cell Biol **141:**397-408.
110. **Saitou, M., M. Furuse, H. Sasaki, J. D. Schulzke, M. Fromm, H. Takano, T. Noda, and S. Tsukita.** 2000. Complex phenotype of mice lacking occludin, a component of tight junction strands. Mol Biol Cell **11:**4131-4142.
111. **Santos-Zavaleta, A., S. Gama-Castro, and E. Perez-Rueda.** A comparative genome analysis of the RpoS-sigmulon shows a high diversity of responses and origins. Microbiology.
112. **Sasakawa, C.** A new paradigm of bacteria-gut interplay brought through the study of Shigella. Proc Jpn Acad Ser B Phys Biol Sci **86:**229-243.
113. **Sason, H., M. Milgrom, A. M. Weiss, N. Melamed-Book, T. Balla, S. Grinstein, S. Backert, I. Rosenshine, and B. Aroeti.** 2009. Enteropathogenic Escherichia coli subverts phosphatidylinositol 4,5-bisphosphate and phosphatidylinositol 3,4,5-trisphosphate upon epithelial cell infection. Mol Biol Cell **20:**544-555.
114. **Savkovic, S. D., J. Villanueva, J. R. Turner, K. A. Matkowskyj, and G. Hecht.** 2005. Mouse model of enteropathogenic Escherichia coli infection. Infect Immun **73:**1161-1170.
115. **Schauer, D. B., and S. Falkow.** 1993. Attaching and effacing locus of a Citrobacter freundii biotype that causes transmissible murine colonic hyperplasia. Infect Immun **61:**2486-2492.
116. **Schauer, D. B., and S. Falkow.** 1993. The eae gene of Citrobacter freundii biotype 4280 is necessary for colonization in transmissible murine colonic hyperplasia. Infect Immun **61:**4654-4661.
117. **Schmitz, H., C. Barmeyer, M. Fromm, N. Runkel, H. D. Foss, C. J. Bentzel, E. O. Riecken, and J. D. Schulzke.** 1999. Altered tight junction structure contributes to the impaired epithelial barrier function in ulcerative colitis. Gastroenterology **116:**301-309.
118. **Schneeberger, E. E., and R. D. Lynch.** 2004. The tight junction: a multifunctional complex. Am J Physiol Cell Physiol **286:**C1213-1228.
119. **Schuller, S., M. Lucas, J. B. Kaper, J. A. Giron, and A. D. Phillips.** 2009. The ex vivo response of human intestinal mucosa to enteropathogenic Escherichia coli infection. Cell Microbiol **11:**521-530.
120. **Shen, L., and J. R. Turner.** 2005. Actin depolymerization disrupts tight junctions via caveolae-mediated endocytosis. Mol Biol Cell **16:**3919-3936.
121. **Shifflett, D. E., D. R. Clayburgh, A. Koutsouris, J. R. Turner, and G. A. Hecht.** 2005. Enteropathogenic E. coli disrupts tight junction barrier function and structure in vivo. Lab Invest **85:**1308-1324.
122. **Shiomi, H., A. Masuda, S. Nishiumi, M. Nishida, T. Takagawa, Y. Shiomi, H. Kutsumi, R. S. Blumberg, T. Azuma, and M. Yoshida.** Gamma interferon produced by

antigen-specific CD4+ T cells regulates the mucosal immune responses to Citrobacter rodentium infection. Infect Immun **78:**2653-2666.

123. **Simmons, C. P., S. Clare, M. Ghaem-Maghami, T. K. Uren, J. Rankin, A. Huett, R. Goldin, D. J. Lewis, T. T. MacDonald, R. A. Strugnell, G. Frankel, and G. Dougan.** 2003. Central role for B lymphocytes and CD4+ T cells in immunity to infection by the attaching and effacing pathogen Citrobacter rodentium. Infect Immun **71:**5077-5086.
124. **Singh, A. K., D. C. Devor, A. C. Gerlach, M. Gondor, J. M. Pilewski, and R. J. Bridges.** 2000. Stimulation of Cl(-) secretion by chlorzoxazone. J Pharmacol Exp Ther **292:**778-787.
125. **Steed, E., M. S. Balda, and K. Matter.** Dynamics and functions of tight junctions. Trends Cell Biol **20:**142-149.
126. **Suzuki, Y. A., K. Shin, and B. Lonnerdal.** 2001. Molecular cloning and functional expression of a human intestinal lactoferrin receptor. Biochemistry **40:**15771-15779.
127. **Tobe, T., and C. Sasakawa.** 2002. Species-specific cell adhesion of enteropathogenic Escherichia coli is mediated by type IV bundle-forming pili. Cell Microbiol **4:**29-42.
128. **Tsuji, S., J. Uehori, M. Matsumoto, Y. Suzuki, A. Matsuhisa, K. Toyoshima, and T. Seya.** 2001. Human intelectin is a novel soluble lectin that recognizes galactofuranose in carbohydrate chains of bacterial cell wall. J Biol Chem **276:**23456-23463.
129. **Umar, S., A. P. Morris, F. Kourouma, and J. H. Sellin.** 2003. Dietary pectin and calcium inhibit colonic proliferation in vivo by differing mechanisms. Cell Prolif **36:**361-375.
130. **Vallance, B. A., W. Deng, K. Jacobson, and B. B. Finlay.** 2003. Host susceptibility to the attaching and effacing bacterial pathogen Citrobacter rodentium. Infect Immun **71:**3443-3453.
131. **Vallance, B. A., W. Deng, L. A. Knodler, and B. B. Finlay.** 2002. Mice lacking T and B lymphocytes develop transient colitis and crypt hyperplasia yet suffer impaired bacterial clearance during Citrobacter rodentium infection. Infect Immun **70:**2070-2081.
132. **van Beelen, A. J., Z. Zelinkova, E. W. Taanman-Kueter, F. J. Muller, D. W. Hommes, S. A. Zaat, M. L. Kapsenberg, and E. C. de Jong.** 2007. Stimulation of the intracellular bacterial sensor NOD2 programs dendritic cells to promote interleukin-17 production in human memory T cells. Immunity **27:**660-669.
133. **Van Itallie, C. M., J. Holmes, A. Bridges, and J. M. Anderson.** 2009. Claudin-2-dependent changes in noncharged solute flux are mediated by the extracellular domains and require attachment to the PDZ-scaffold. Ann N Y Acad Sci **1165:**82-87.
134. **Viau, C., V. Le Sage, D. K. Ting, J. Gross, and H. Le Moual.** Absence of PmrAB-mediated phosphoethanolamine modifications of Citrobacter rodentium lipopolysaccharide affects outer membrane integrity. J Bacteriol.
135. **Viswanathan, V. K., K. Hodges, and G. Hecht.** 2009. Enteric infection meets intestinal function: how bacterial pathogens cause diarrhoea. Nat Rev Microbiol **7:**110-119.
136. **Vogelmann, R., M. R. Amieva, S. Falkow, and W. J. Nelson.** 2004. Breaking into the epithelial apical-junctional complex--news from pathogen hackers. Curr Opin Cell Biol **16:**86-93.
137. **Von Moll, L. K., and J. R. Cantey.** 1997. Peyer's patch adherence of enteropathogenic Escherichia coli strains in rabbits. Infect Immun **65:**3788-3793.

138. **Watson, C. J., C. J. Hoare, D. R. Garrod, G. L. Carlson, and G. Warhurst.** 2005. Interferon-gamma selectively increases epithelial permeability to large molecules by activating different populations of paracellular pores. J Cell Sci **118:**5221-5230.
139. **Weber, G. F., M. A. Bjerke, and D. W. Desimone.** Integrins and cadherins join forces to form adhesive networks. J Cell Sci **124:**1183-1193.
140. **Wei, O. L., A. Hilliard, D. Kalman, and M. Sherman.** 2005. Mast cells limit systemic bacterial dissemination but not colitis in response to Citrobacter rodentium. Infect Immun **73:**1978-1985.
141. **Whitehead, R. H., P. S. Robinson, J. A. Williams, W. Bie, A. L. Tyner, and J. L. Franklin.** 2008. Conditionally immortalized colonic epithelial cell line from a Ptk6 null mouse that polarizes and differentiates in vitro. J Gastroenterol Hepatol **23:**1119-1124.
142. **Wiles, S., S. Clare, J. Harker, A. Huett, D. Young, G. Dougan, and G. Frankel.** 2004. Organ specificity, colonization and clearance dynamics in vivo following oral challenges with the murine pathogen Citrobacter rodentium. Cell Microbiol **6:**963-972.
143. **Wintermute, E. H., and P. A. Silver.** Dynamics in the mixed microbial concourse. Genes Dev **24:**2603-2614.
144. **Wu, X., B. A. Vallance, L. Boyer, K. S. Bergstrom, J. Walker, K. Madsen, J. R. O'Kusky, A. M. Buchan, and K. Jacobson.** 2008. Saccharomyces boulardii ameliorates Citrobacter rodentium-induced colitis through actions on bacterial virulence factors. Am J Physiol Gastrointest Liver Physiol **294:**G295-306.
145. **Yamazaki, Y., K. Okawa, T. Yano, and S. Tsukita.** 2008. Optimized proteomic analysis on gels of cell-cell adhering junctional membrane proteins. Biochemistry **47:**5378-5386.
146. **Yang, J., M. Tauschek, E. Hart, E. L. Hartland, and R. M. Robins-Browne.** Virulence regulation in Citrobacter rodentium: the art of timing. Microb Biotechnol **3:**259-268.
147. **Yoshida, M., K. Kobayashi, T. T. Kuo, L. Bry, J. N. Glickman, S. M. Claypool, A. Kaser, T. Nagaishi, D. E. Higgins, E. Mizoguchi, Y. Wakatsuki, D. C. Roopenian, A. Mizoguchi, W. I. Lencer, and R. S. Blumberg.** 2006. Neonatal Fc receptor for IgG regulates mucosal immune responses to luminal bacteria. J Clin Invest **116:**2142-2151.
148. **Yu, D., and J. R. Turner.** 2008. Stimulus-induced reorganization of tight junction structure: the role of membrane traffic. Biochim Biophys Acta **1778:**709-716.
149. **Yu, F. S., M. D. Cornicelli, M. A. Kovach, M. W. Newstead, X. Zeng, A. Kumar, N. Gao, S. G. Yoon, R. L. Gallo, and T. J. Standiford.** Flagellin stimulates protective lung mucosal immunity: role of cathelicidin-related antimicrobial peptide. J Immunol **185:**1142-1149.
150. **Zachos, N. C., M. Tse, and M. Donowitz.** 2005. Molecular physiology of intestinal Na+/H+ exchange. Annu Rev Physiol **67:**411-443.
151. **Zanetti, M.** 2004. Cathelicidins, multifunctional peptides of the innate immunity. J Leukoc Biol **75:**39-48.
152. **Zeissig, S., N. Burgel, D. Gunzel, J. Richter, J. Mankertz, U. Wahnschaffe, A. J. Kroesen, M. Zeitz, M. Fromm, and J. D. Schulzke.** 2007. Changes in expression and distribution of claudin 2, 5 and 8 lead to discontinuous tight junctions and barrier dysfunction in active Crohn's disease. Gut **56:**61-72.

153. **Zhang, Q., Q. Li, C. Wang, X. Liu, N. Li, and J. Li.** Enteropathogenic Escherichia coli changes distribution of occludin and ZO-1 in tight junction membrane microdomains in vivo. Microb Pathog **48:**28-34.
154. **Zheng, Y., P. A. Valdez, D. M. Danilenko, Y. Hu, S. M. Sa, Q. Gong, A. R. Abbas, Z. Modrusan, N. Ghilardi, F. J. de Sauvage, and W. Ouyang.** 2008. Interleukin-22 mediates early host defense against attaching and effacing bacterial pathogens. Nat Med **14:**282-289.